

# Recent Development of Multiscale Data Assimilation for Numerical Weather Prediction

---

**Xuguang Wang**

**M**ultiscale data **A**ssimilation and **P**redictability (**MAP**) lab  
University of Oklahoma, Norman, USA

## **Acknowledgement**

Yongming Wang\*, Erin Jones\*, Xu Lu\*, Naicheng Xu\*, Yue Yang\* (OU MAP)  
Collaborators from NOAA EMC, PSL, GSL, HRD, NSSL; NRL; Univ. Melbourne

\*MAP lab students/early career scientists

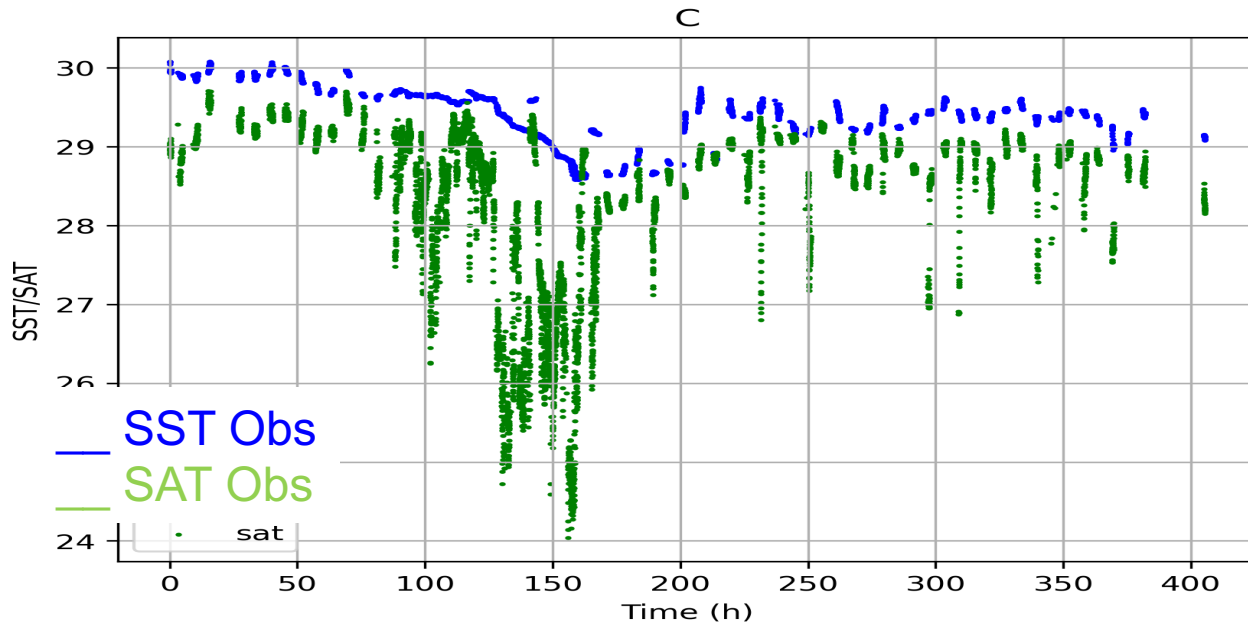




<https://www.ecmwf.int/en/about/media-centre/focus/2021/fact-sheet-earth-system-modelling-ecmwf>

- ❑ In addition to the atmosphere, ocean, sea ice, and the land surface etc can have a significant impact on weather.
- ❑ These earth system components have **intrinsically different spatial and temporal scales**.
- ❑ Accurate numerical weather prediction requires proper initialization of these **multiscale** earth system components and their **interaction (coupling)** through data assimilation.

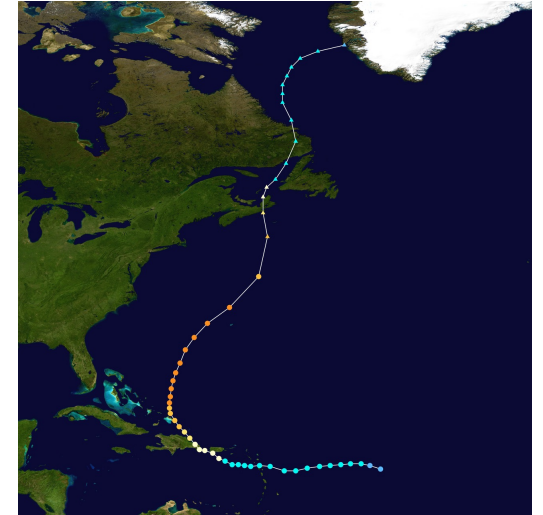
# Why Multiscale Data Assimilation (MDA)



Lu\* and Wang et al. 2023b



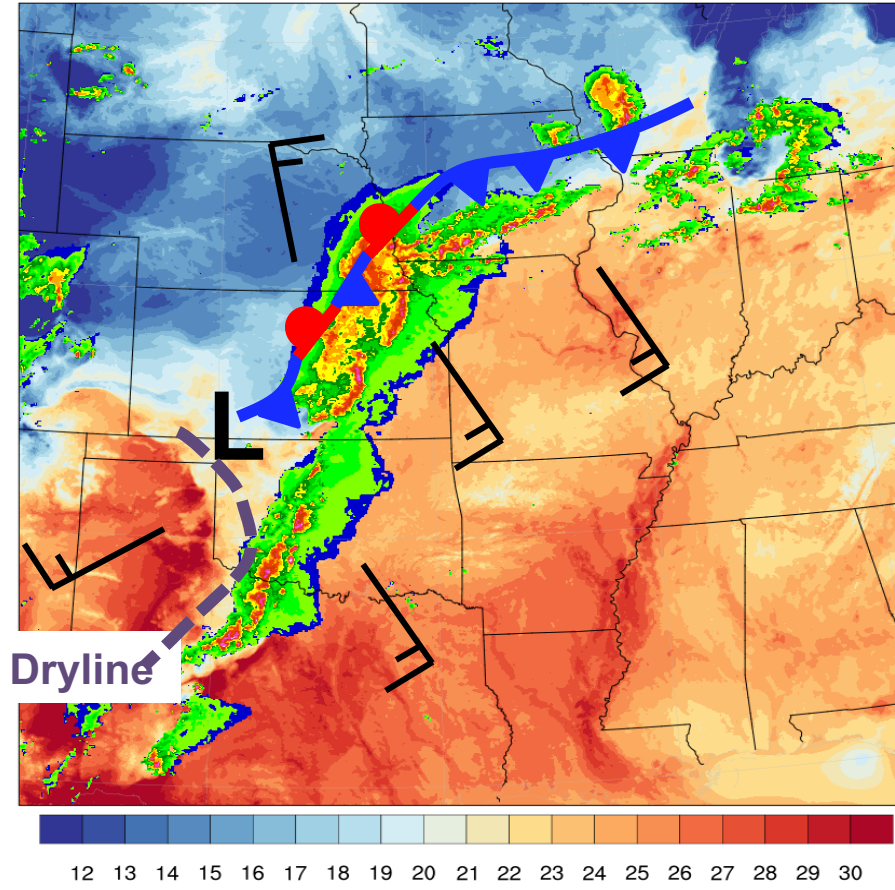
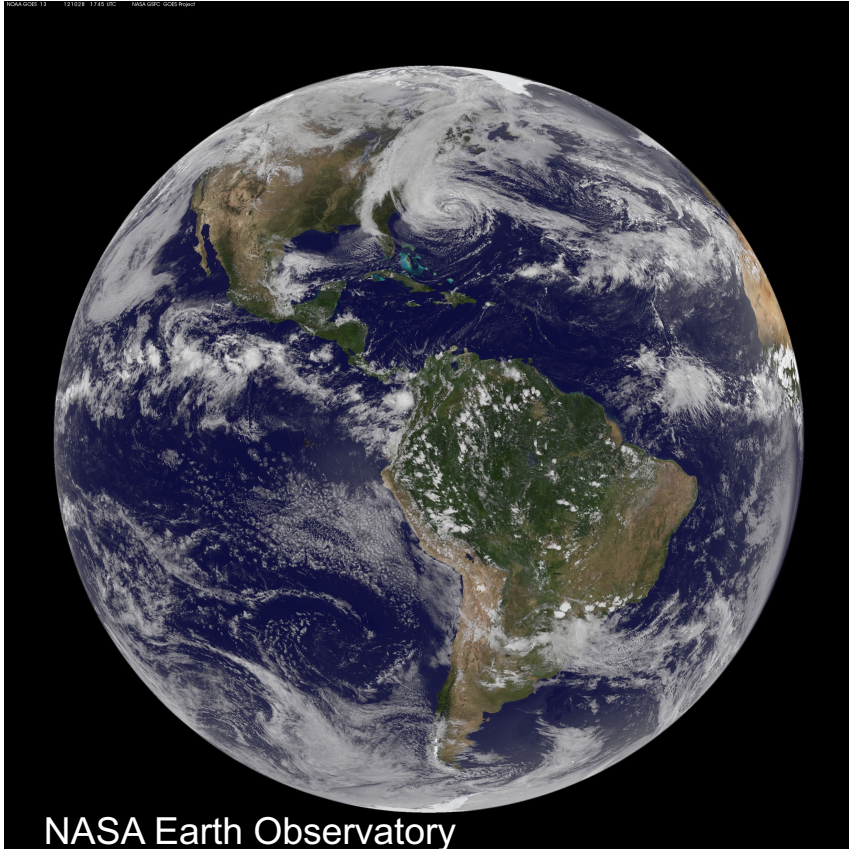
Saildrone.com



[https://en.wikipedia.org/wiki/Hurricane\\_Fiona](https://en.wikipedia.org/wiki/Hurricane_Fiona)

- Proper initialization of earth system components and their interactions (coupling) through MDA not only applies for e.g. S2S prediction, but also for short term prediction.

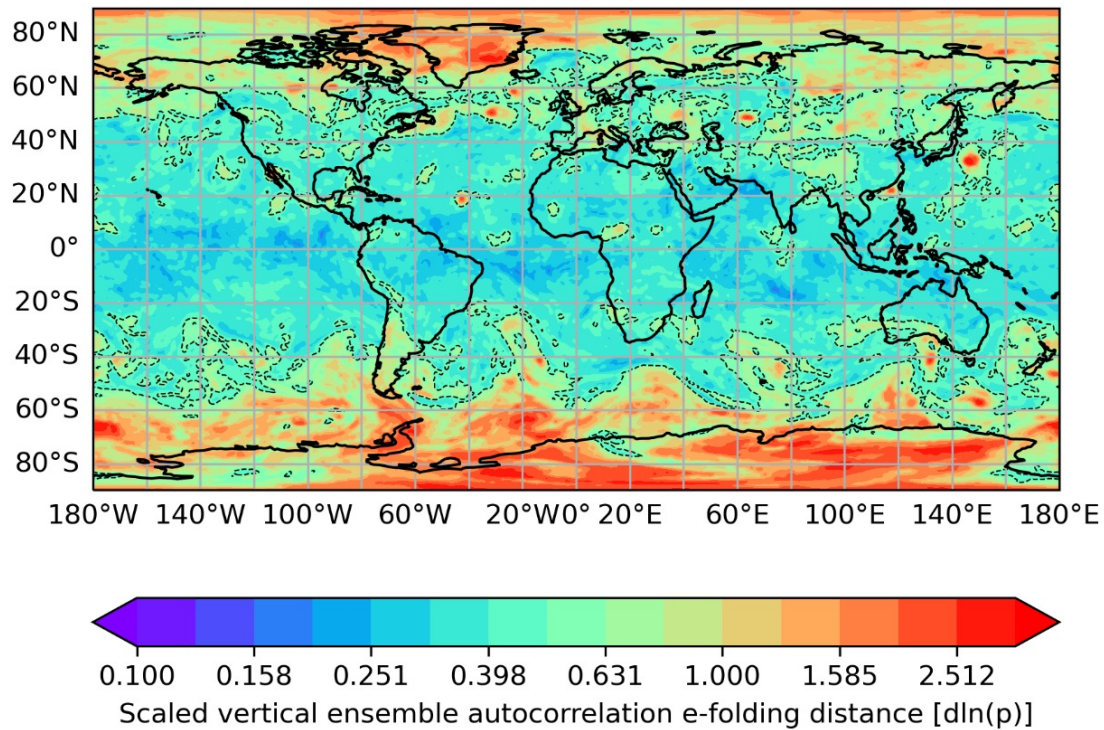
# Why Multiscale Data Assimilation (MDA)



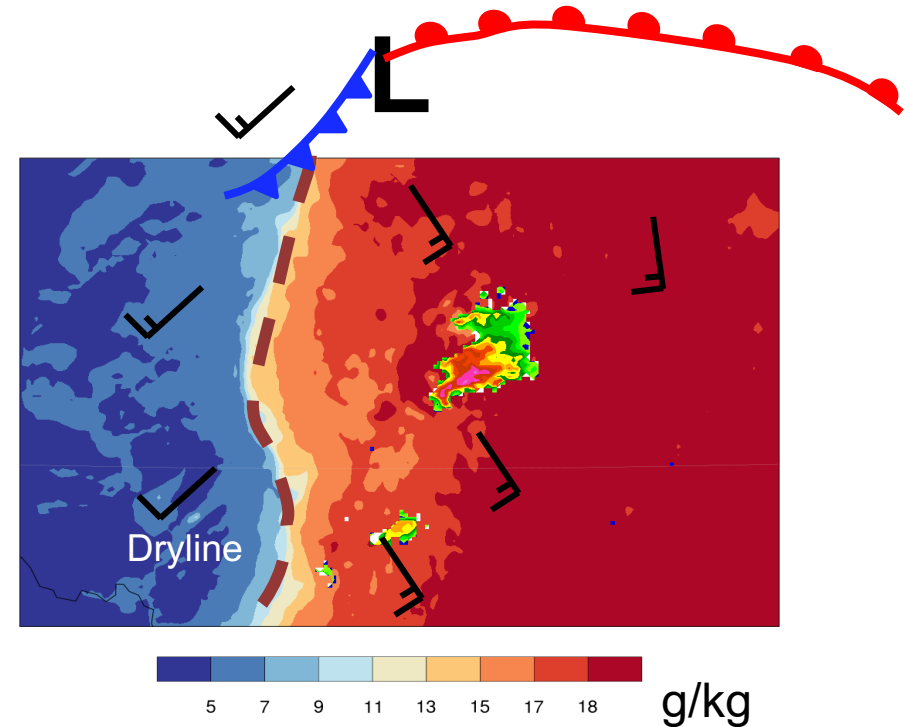
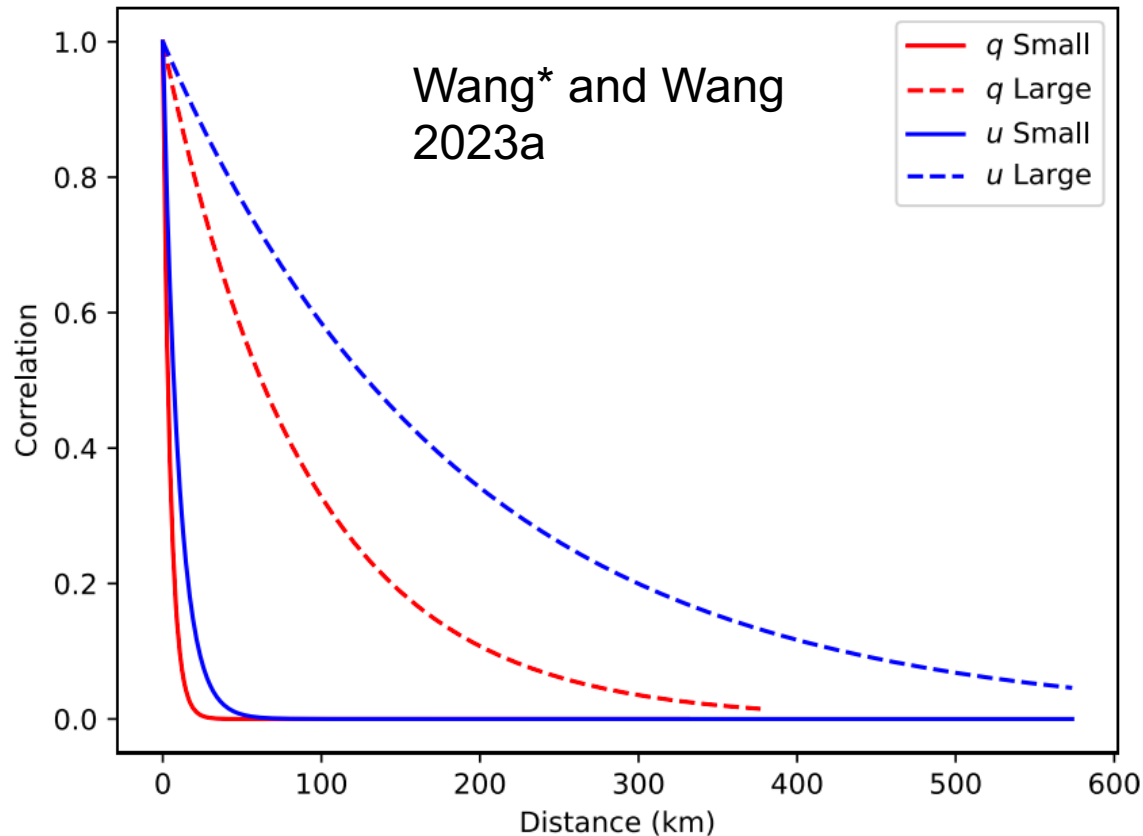
Wang\* and Wang, 2023b

- The atmosphere, as one earth system component, itself is intrinsically multiscale as well, housing micro to planetary scales.
- Accurate prediction of storms (e.g. hurricanes, squall lines, supercells) require DA to initialize not only the storm but also its larger scale environment.

Jones\* and Wang 2023b



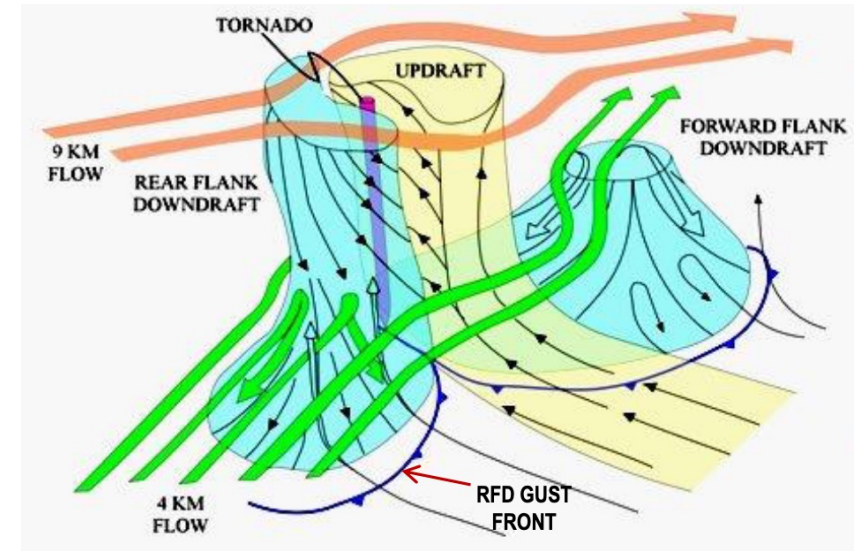
- ❑ Deep convective systems have larger vertical correlation length scales than the mean atmospheric state (e.g., Ingleby 2001)
- ❑ Mean tropical atmosphere has smaller vertical correlation length than extratropics (e.g., Rabier et al. 1998)



- Different variables can have intrinsically different scales.
- Considering intrinsic scale differences of variables are important for storm scale prediction (Wang, Y.\* and X. Wang 2023)

- Control variables and intrinsic “balance” are different between large scales and convective scales

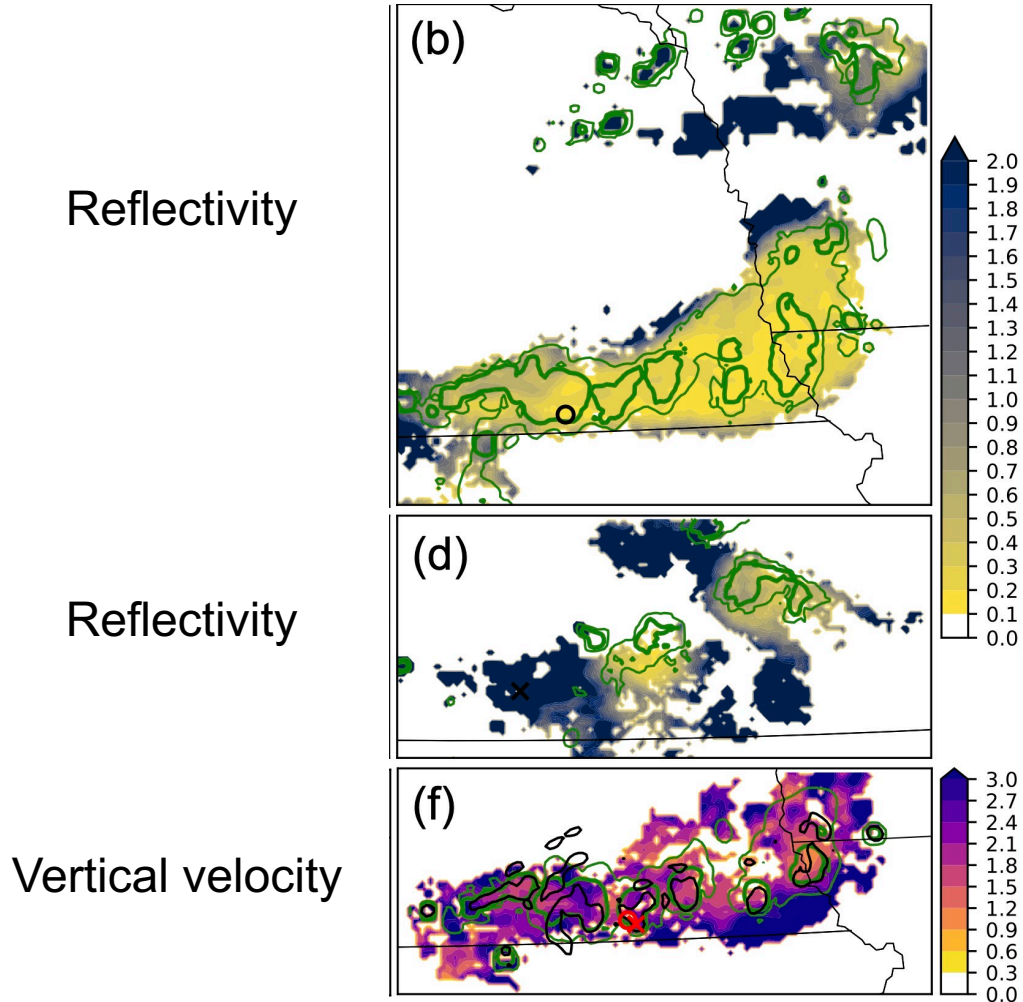
$$\begin{pmatrix} u \\ v \\ t \\ ps \\ rh \\ w \\ ql \\ qr \\ qs \\ qi \\ qg \\ dbz \end{pmatrix} = \begin{pmatrix} \mathbf{I} & 0 & 0 & 0 & 0 & 0 & 0 & 0 & 0 & 0 & 0 & 0 \\ \mathbf{r}_{11} & \mathbf{I} & 0 & 0 & 0 & 0 & 0 & 0 & 0 & 0 & 0 & 0 \\ \mathbf{r}_{21} & \mathbf{r}_{22} & \mathbf{I} & 0 & 0 & 0 & 0 & 0 & 0 & 0 & 0 & 0 \\ \mathbf{r}_{31} & \mathbf{r}_{32} & \mathbf{r}_{33} & \mathbf{I} & 0 & 0 & 0 & 0 & 0 & 0 & 0 & 0 \\ \mathbf{r}_{41} & \mathbf{r}_{42} & \mathbf{r}_{43} & \mathbf{r}_{44} & \mathbf{I} & 0 & 0 & 0 & 0 & 0 & 0 & 0 \\ \mathbf{r}_{51} & \mathbf{r}_{52} & \mathbf{r}_{53} & \mathbf{r}_{54} & \mathbf{r}_{55} & \mathbf{I} & 0 & 0 & 0 & 0 & 0 & 0 \\ \mathbf{r}_{61} & \mathbf{r}_{62} & \mathbf{r}_{63} & \mathbf{r}_{64} & \mathbf{r}_{65} & \mathbf{r}_{66} & \mathbf{I} & 0 & 0 & 0 & 0 & 0 \\ \mathbf{r}_{71} & \mathbf{r}_{72} & \mathbf{r}_{73} & \mathbf{r}_{74} & \mathbf{r}_{75} & \mathbf{r}_{76} & \mathbf{r}_{77} & \mathbf{I} & 0 & 0 & 0 & 0 \\ \mathbf{r}_{81} & \mathbf{r}_{82} & \mathbf{r}_{83} & \mathbf{r}_{84} & \mathbf{r}_{85} & \mathbf{r}_{86} & \mathbf{r}_{87} & \mathbf{r}_{88} & \mathbf{I} & 0 & 0 & 0 \\ \mathbf{r}_{91} & \mathbf{r}_{92} & \mathbf{r}_{93} & \mathbf{r}_{94} & \mathbf{r}_{95} & \mathbf{r}_{96} & \mathbf{r}_{97} & \mathbf{r}_{98} & \mathbf{r}_{99} & \mathbf{I} & 0 & 0 \\ \mathbf{r}_{101} & \mathbf{r}_{102} & \mathbf{r}_{103} & \mathbf{r}_{104} & \mathbf{r}_{105} & \mathbf{r}_{106} & \mathbf{r}_{107} & \mathbf{r}_{108} & \mathbf{r}_{109} & \mathbf{r}_{1010} & \mathbf{I} & 0 \\ \mathbf{r}_{111} & \mathbf{r}_{112} & \mathbf{r}_{113} & \mathbf{r}_{114} & \mathbf{r}_{115} & \mathbf{r}_{116} & \mathbf{r}_{117} & \mathbf{r}_{118} & \mathbf{r}_{119} & \mathbf{r}_{1110} & \mathbf{r}_{1111} & \mathbf{I} \end{pmatrix} \begin{pmatrix} u \\ v_u \\ t_u \\ ps_u \\ rh_u \\ w_u \\ ql_u \\ qr_u \\ qs_u \\ qi_u \\ qg_u \\ dbz_u \end{pmatrix}$$



Convective scale static B  
Wang Y.\* and X. Wang 2021

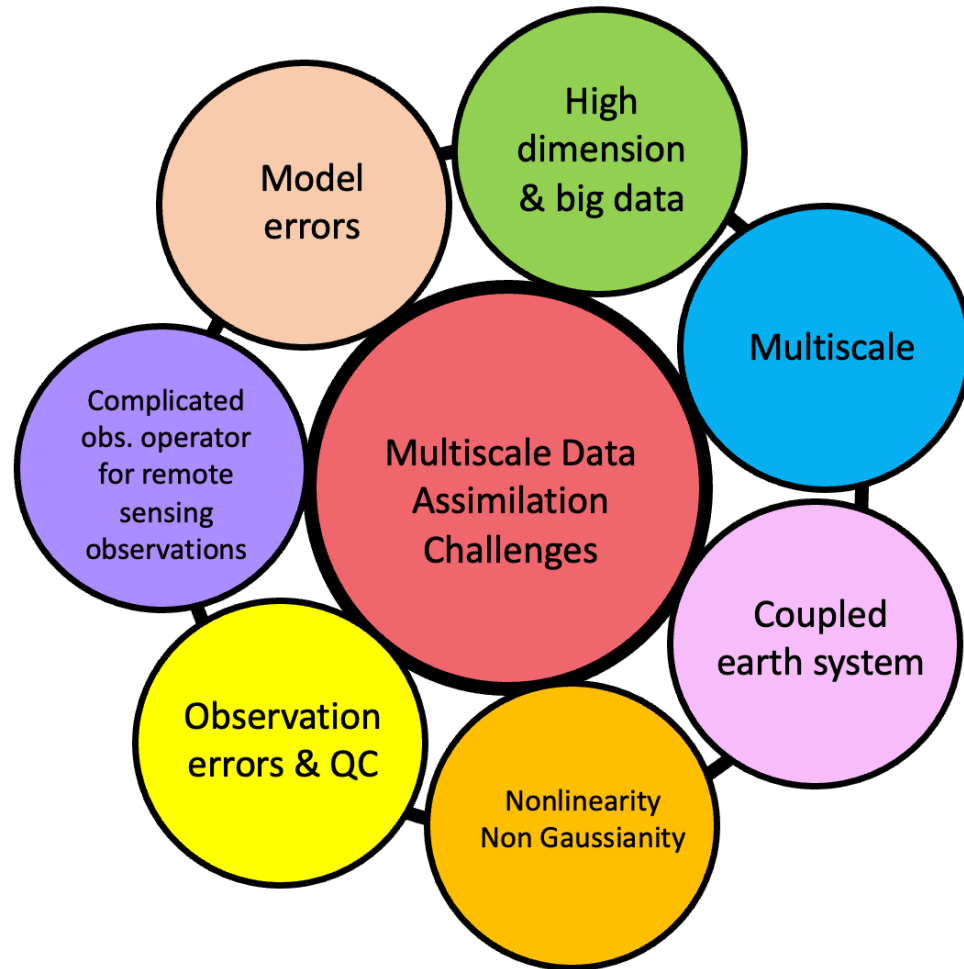
[[https://www.weather.gov/media/lmk/soo/Su\\_perccell\\_Structure.pdf](https://www.weather.gov/media/lmk/soo/Su_perccell_Structure.pdf)]

Non-Gaussianity  $D_{KL}$



- Degrees of Non-Gaussianity/Non-linearity may be scale dependent





- The next generation data assimilation system is required to **effectively analyze the state and quantify its uncertainty across multiple scales**, termed as “multiscale data assimilation (MDA)”.



# OU MAP Lab current MDA efforts



- MDA methodology development
  - **Develop new simultaneous MDA algorithm/solver:** e.g. MLGETKF (Wang, X. et al. 2021)
  - **Develop methods to address ensemble deficiency for simultaneous MDA**
    - ✓ Scale dependent inflation (SDI, Xu\* et al. 2023)
    - ✓ Scale dependent horizontal localization (SDL, Huang\* et al. 2021, Lu\* and Wang 2023)
    - ✓ Scale dependent/flow dependent vertical localization (vFDL, Jones\* and Wang 2023b)
    - ✓ Variable dependent localization (VDL, Wang\* and Wang 2023a)
    - ✓ Multi-resolution (MR) background ensemble (Kay\* and Wang 2020, Jones\* and Wang 2023a)
    - ✓ Optimizing coupled earth system component covariances, e.g. air-sea coupling for TC (Lu\* et al. 2023)



# OU MAP Lab current MDA efforts



- R&D of MDA for real NWP applications in US NOAA DA systems
  - MR and SDL for **GFS** 4DEnVar (Kay\* and Wang 2020, Huang\* et al. 2021, Jones\* and Wang 2023a)
  - SDLVDL for **HRRR/RRFS** and **WoF** EnVar (Wang\* and Wang 2023ab)
  - SDL for **HAFS** EnVar (Lu\* and Wang 2023)
  - Coupled DA for **HAFS-MOM6** (Lu\* et al. 2003)

**GFS**: US operational global model

**HRRR/RRFS**: US current and next generation convection allowing DA and modeling system over CONUS

**HAFS**: US next generation convection allowing hurricane DA and modeling system

**WoF**: US experimental DA and modeling system for tornado, severe thunderstorm, etc



# Part I: A Multi-Resolution (MR) Ensemble 4DEnVar for GFS

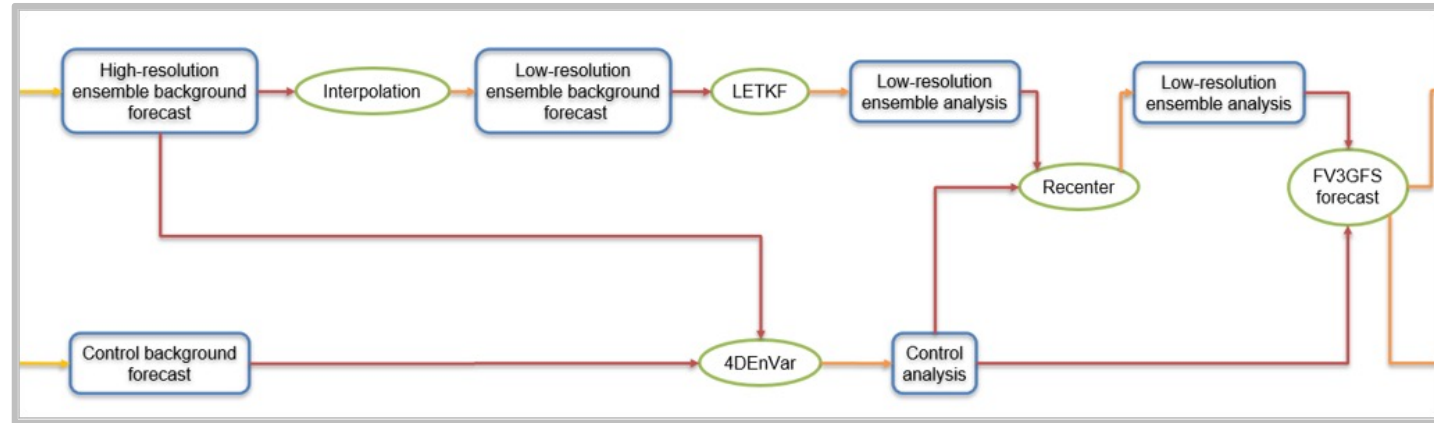


Kay\* and Wang, 2020; Jones\* and Wang, 2023a

## Hybrid 4DEnVar (Wang and Lei\* 2014)

$$\begin{aligned}
 & J[(\mathbf{x}'_1)_t, \boldsymbol{\alpha}] \\
 &= \frac{1}{2} \beta_1 (\mathbf{x}'_1)_t^T \mathbf{B}_1^{-1} (\mathbf{x}'_1)_t + \frac{1}{2} \beta_e (\boldsymbol{\alpha})^T \mathbf{A}^{-1} (\boldsymbol{\alpha}) \\
 &+ \frac{1}{2} \sum_{t=1}^L (\mathbf{H}\mathbf{x}'_t - \mathbf{y}_t^o)^T \mathbf{R}^{-1} (\mathbf{H}\mathbf{x}'_t - \mathbf{y}_t^o)
 \end{aligned}$$

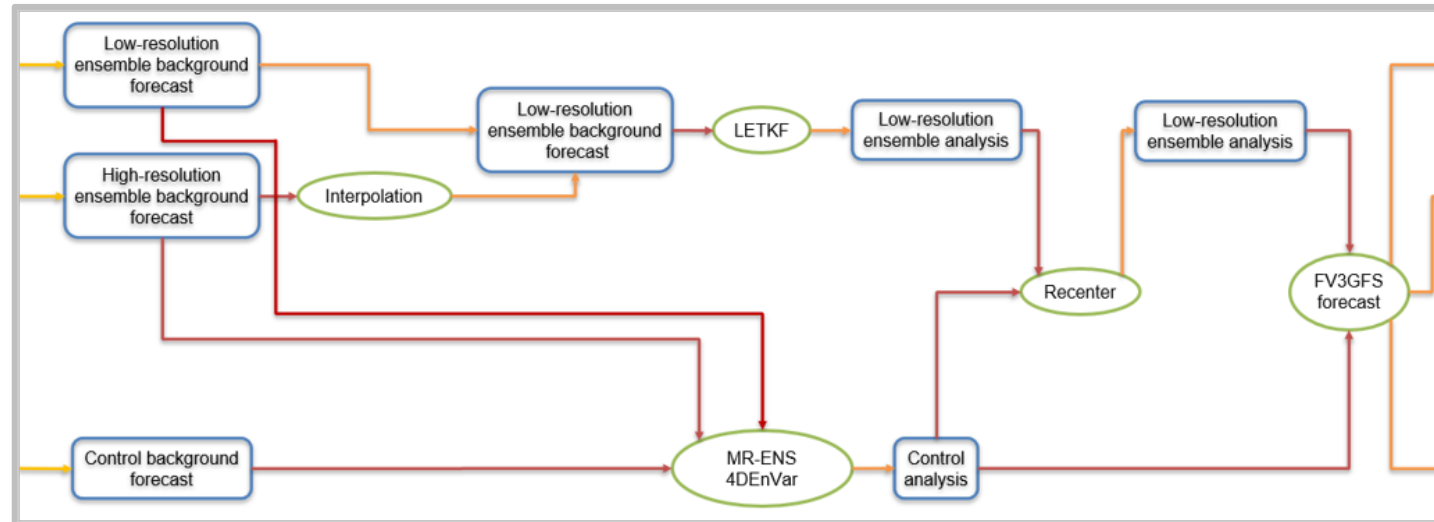
Single-scale localization (pointing to  $\mathbf{A}^{-1}(\boldsymbol{\alpha})$ )  
 single-res ensemble (under the second term)



## Multi-resolution ensemble (Kay\* and Wang 2020) hybrid 4DEnVar

$$\begin{aligned}
 & J[(\mathbf{x}'_1)_t, \boldsymbol{\alpha}^L, \boldsymbol{\alpha}^H] \\
 &= \frac{1}{2} \beta_1 (\mathbf{x}'_1)_t^T \mathbf{B}_1^{-1} (\mathbf{x}'_1)_t + \frac{1}{2} \beta_L (\boldsymbol{\alpha}^L)^T \mathbf{A}_L^{-1} (\boldsymbol{\alpha}^L) \\
 &+ \frac{1}{2} \beta_H (\boldsymbol{\alpha}^H)^T \mathbf{A}_H^{-1} (\boldsymbol{\alpha}^H) \\
 &+ \frac{1}{2} \sum_{t=1}^L (\mathbf{H}\mathbf{x}'_t - \mathbf{y}_t^o)^T \mathbf{R}^{-1} (\mathbf{H}\mathbf{x}'_t - \mathbf{y}_t^o)
 \end{aligned}$$

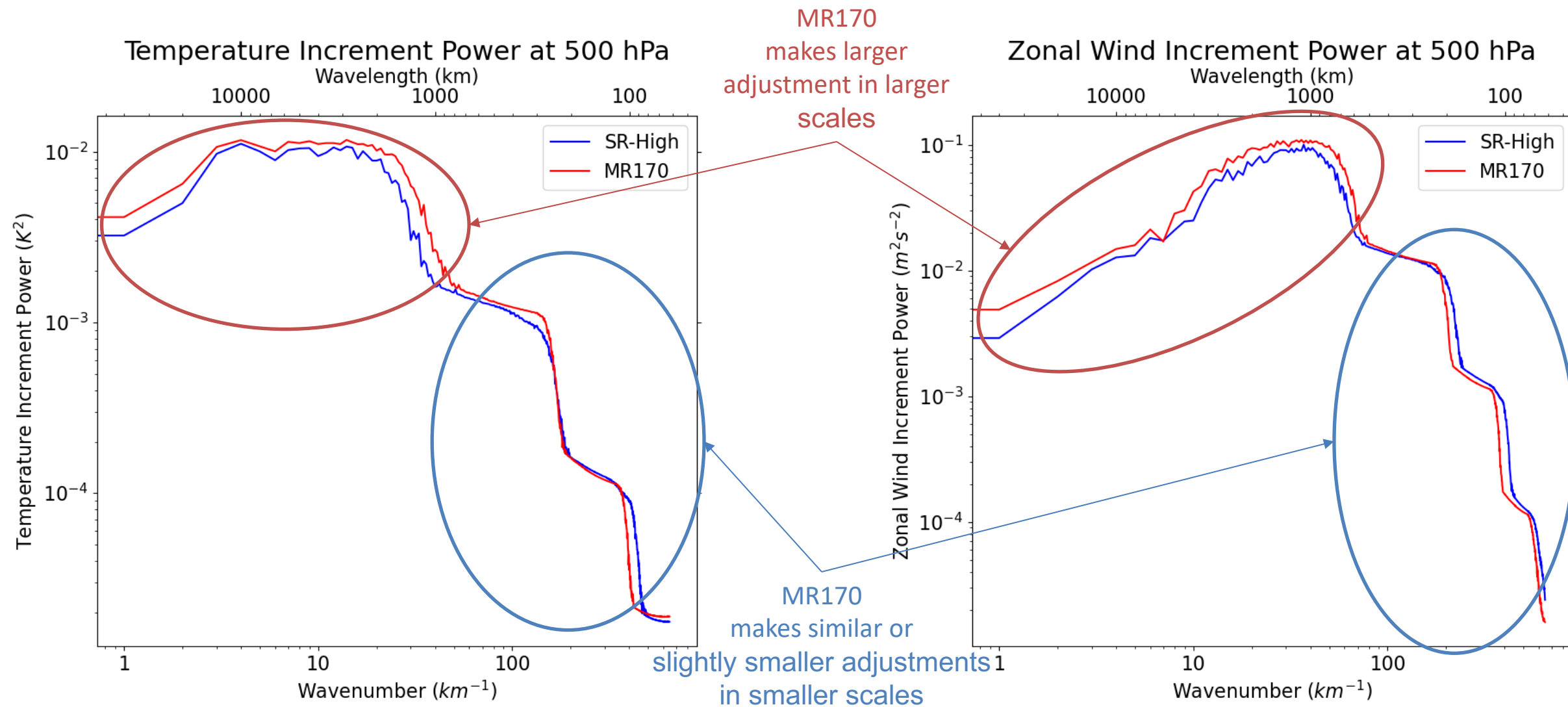
Large localization radius applied for low-res ensemble (pointing to  $\mathbf{A}_L^{-1}(\boldsymbol{\alpha}^L)$ )  
 low-res ensemble (under the second term)  
 Small localization radius applied for high-res ensemble (pointing to  $\mathbf{A}_H^{-1}(\boldsymbol{\alpha}^H)$ )  
 high-res ensemble (under the third term)





# Analysis Increment Power Spectrum

Jones\* and Wang, 2023a





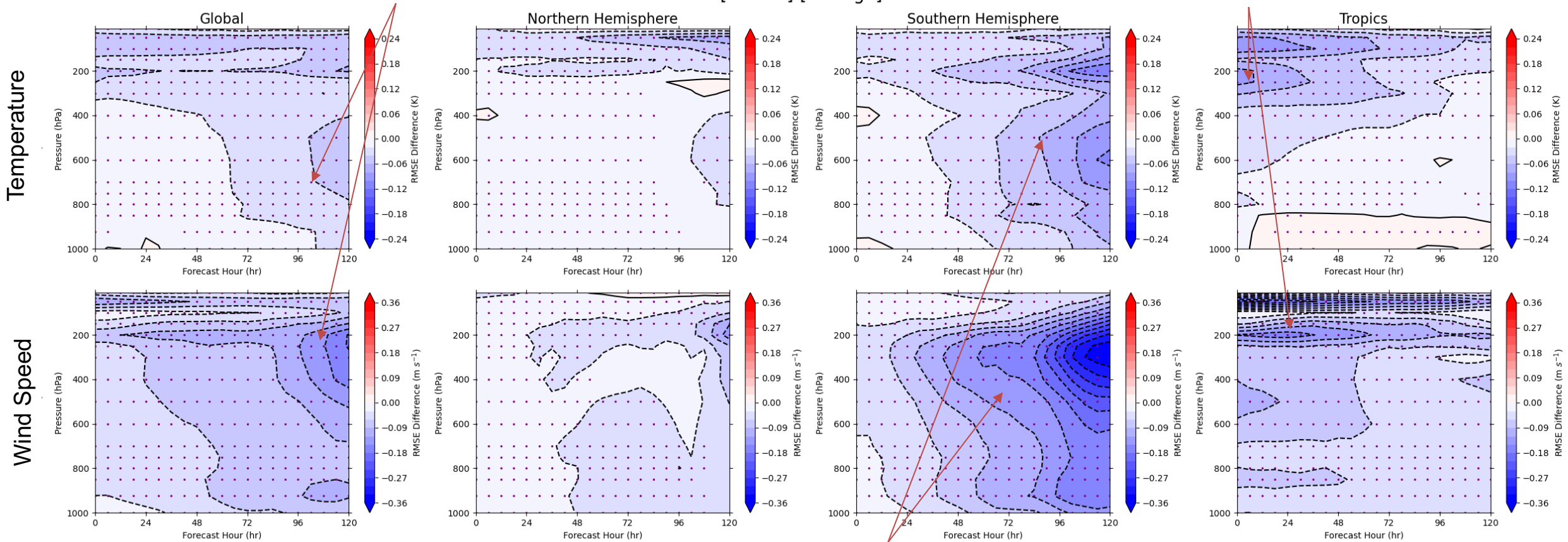
# Impact on GFS forecast RMSE from cycled NH summer month long experiment



MR170 improves global forecast compared with SR-High up to 5 days

Root Mean Square Error Differences [MR170]-[SR-High]

Improvement at early lead times is most notable in the Tropics



Improvement at longer lead times is most notable in the Southern Hemisphere

Error calculated using ERA-Interim as verification. Purple asterisks indicate 95% confidence using a paired *t*-test.

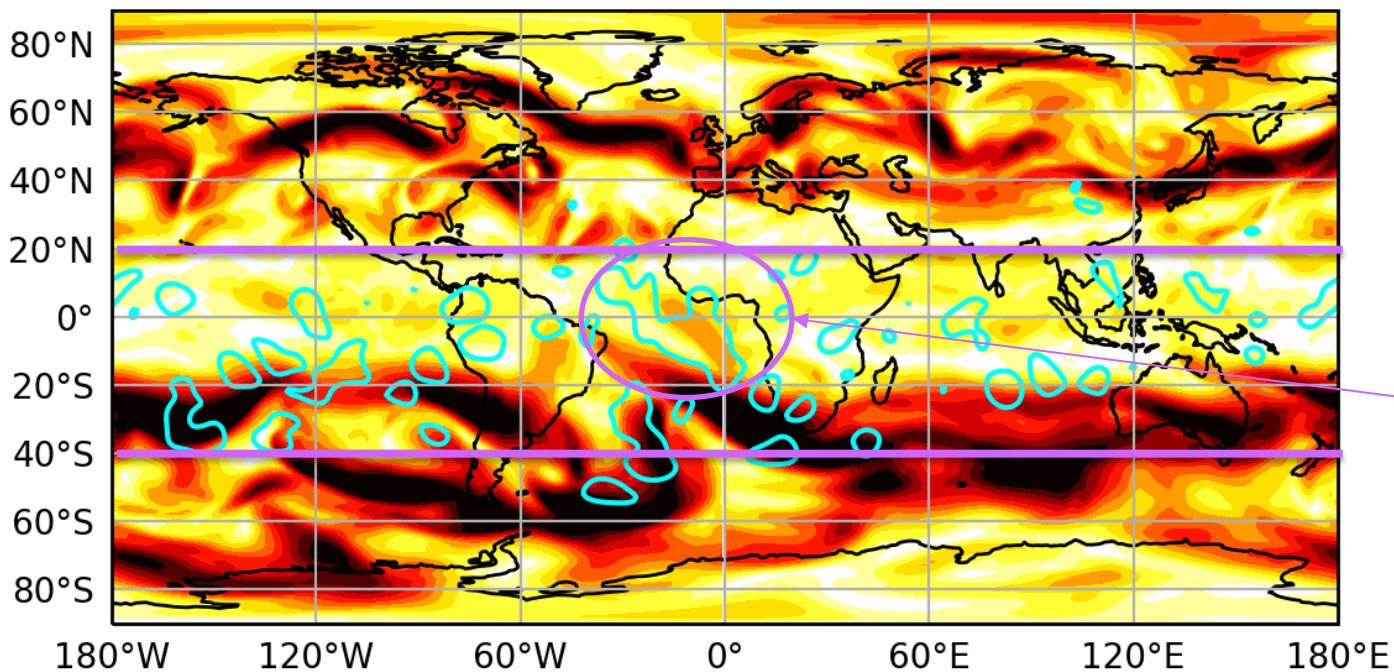


# Why Multi-Resolution (MR) Ensemble 4DEnVar helps?



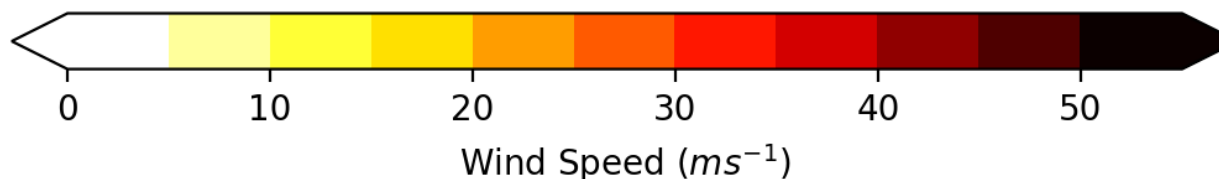
250 hPa Wind Speed and Difference in Total Energy Error

0 hrs



At analysis time, largest MR170 improvement in the tropics and SH subtropics

Largest area of improvement in region typically associated with Tropical Easterly Jet



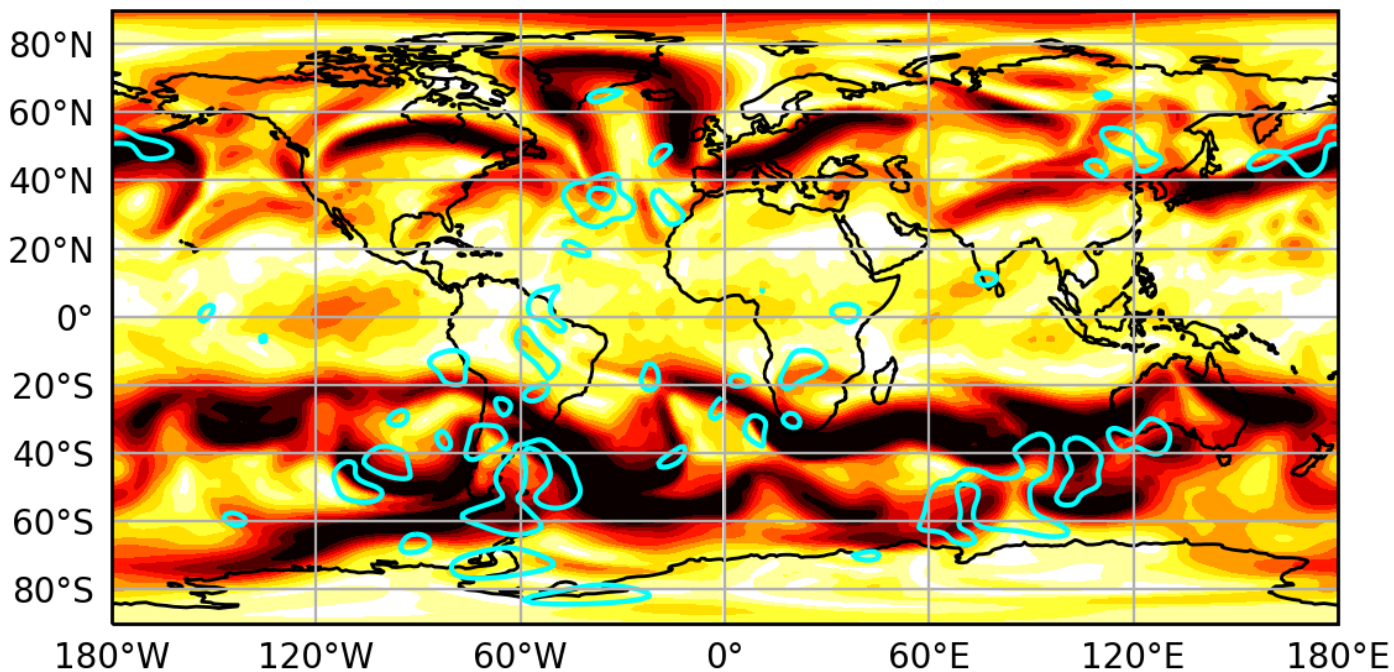
Analysis time: 0000 UTC on 12 September 2017. Cyan contours indicate the 5% maximum improvement of total energy error filtered to include wavenumbers 5 to 25 for MR170 compared with SR-High



# Why Multi-Resolution (MR) 4DEnVar helps?

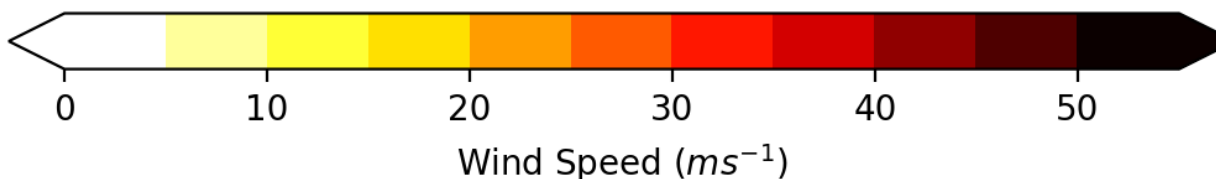


72 hrs



Largest MR170 improvement shifts to extratropics, especially in SH

Largest areas of improvement tend to occur in regions influenced by jet interactions



Analysis time: 0000 UTC on 12 September 2017. Cyan contours indicate the 5% maximum improvement of total energy error filtered to include wavenumbers 5 to 25 for MR170 compared with SR-High





# Part II: Simultaneous MDA with scale dependent localization (SDL) in GFS and HAFS 4DEnVar

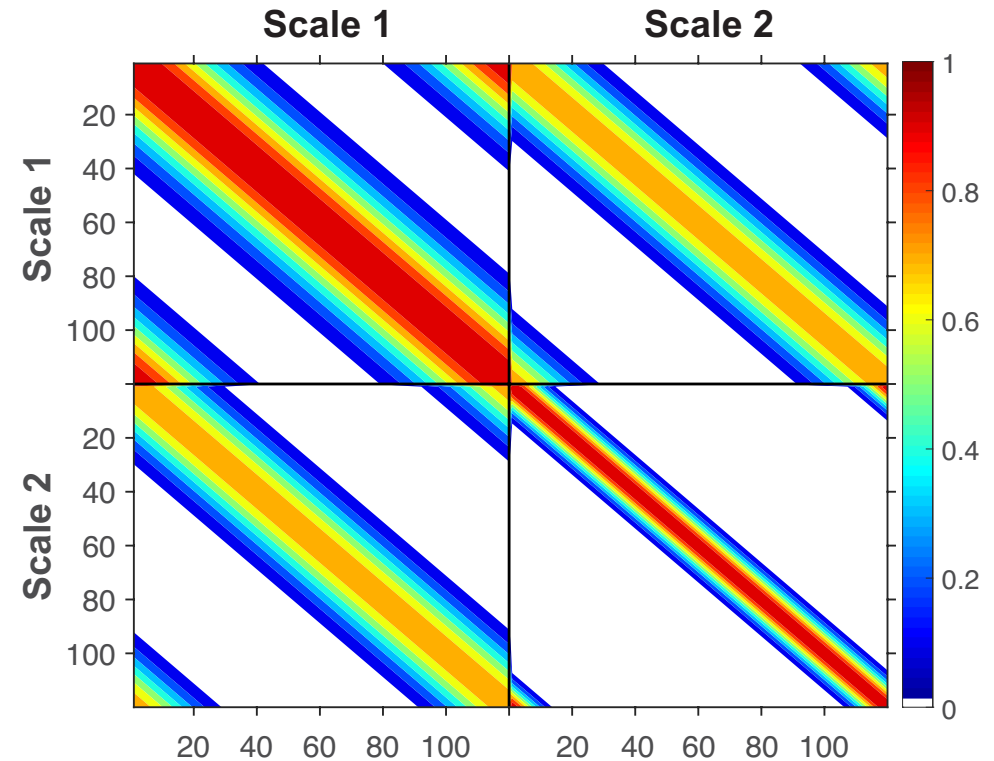
Huang\* et al. 2021, Lu\* and Wang 2023



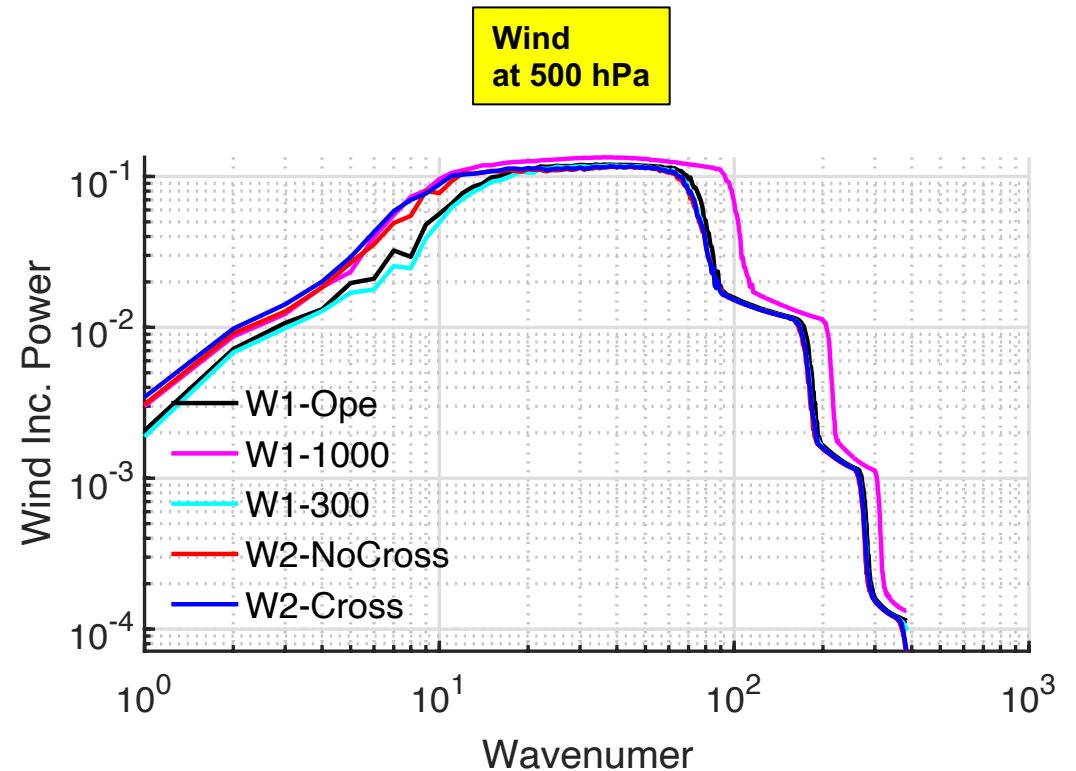
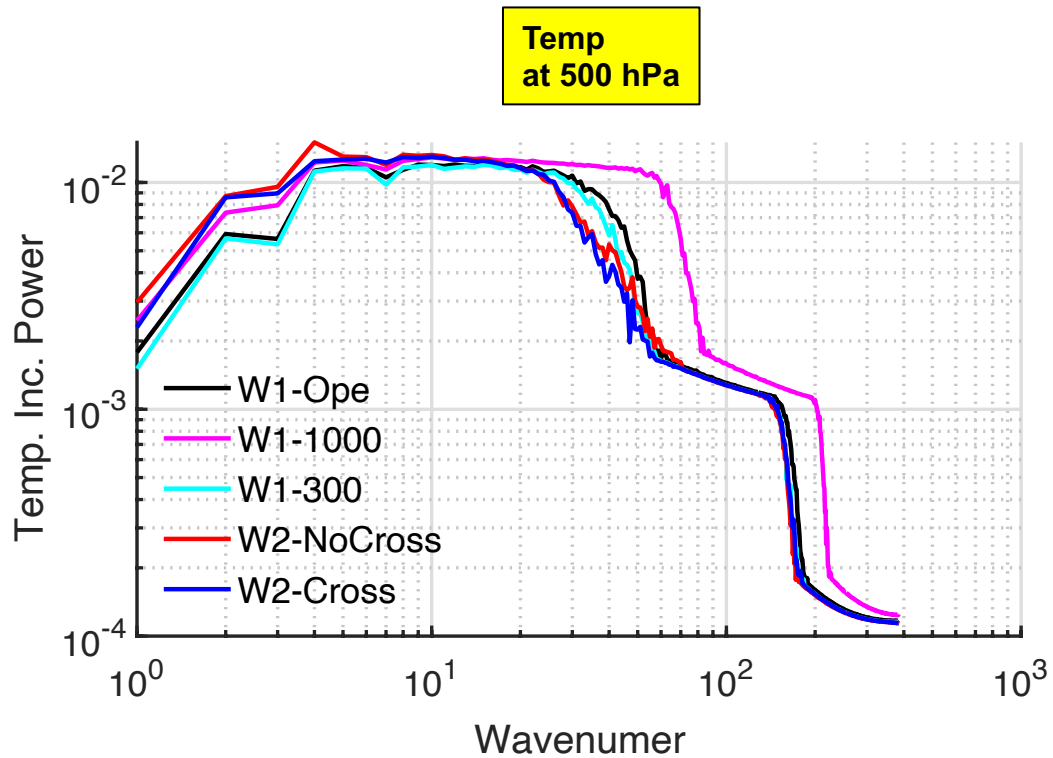
- ❑ In the operational 4DEnVar, horizontal localization functions are scale-invariant at each level
- ❑ A simultaneous multiscale DA using scale dependent localization (SDL, Buehner and Shlyayeva 2015) in 4DEnVar for NCEP FV3-based GFS is implemented

- ensemble perturbation scale decomposition;
- scale dependent and cross scale covariance localization

$$J(\mathbf{x}'_1, \hat{\mathbf{a}}) = \frac{1}{2} \beta_1 (\mathbf{x}'_1)^T \mathbf{B}_1^{-1} (\mathbf{x}'_1) + \frac{1}{2} \beta_2 (\hat{\mathbf{a}})^T \hat{\mathbf{A}}^{-1} (\hat{\mathbf{a}}) + \frac{1}{2} \sum_{t=1}^L (\mathbf{y}_t^{o'} - \mathbf{H}_t \mathbf{x}'_t)^T \mathbf{R}_t^{-1} (\mathbf{y}_t^{o'} - \mathbf{H}_t \mathbf{x}'_t),$$



# Analysis Increment Power



- ❑ By comparing W1 experiments, wider localization length results in larger analysis increment power.
- ❑ As expected, analysis increment power in W2-NoCross and W2-Cross is closer to W1-1000 (W1-300) at small (large) total wavenumbers -> **MDA with SDL can simultaneously update large and small scales**

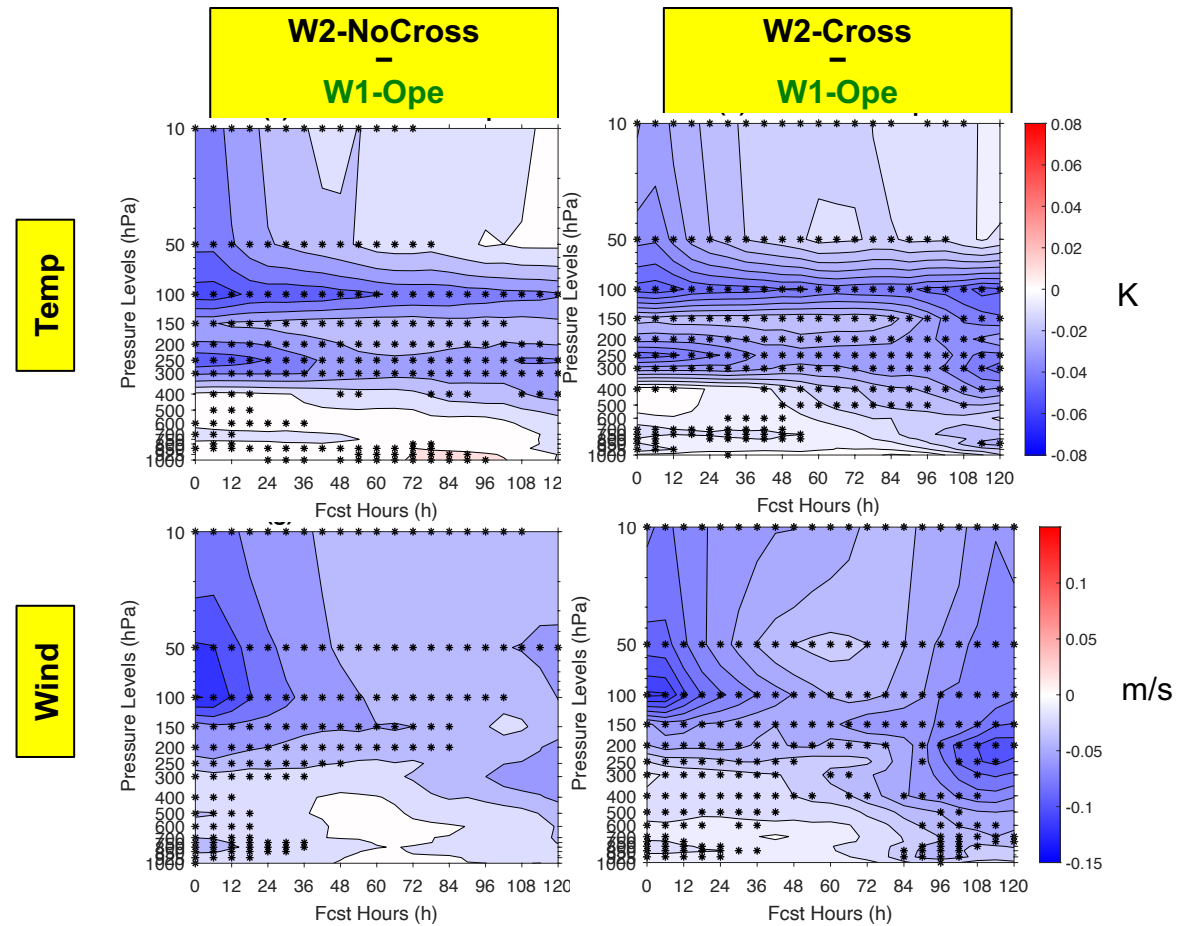


# Impact on GFS forecast from month long cycled experiments



RMSE difference (blue/red → improvement/degradation relative to W1-Ope)

- ❑ MDA with SDL improves global forecasts almost at all pressure levels over operational approach.
- ❑ NOAA pre-implementation test shows similar global forecast improvement (Kleist et al. 2023)

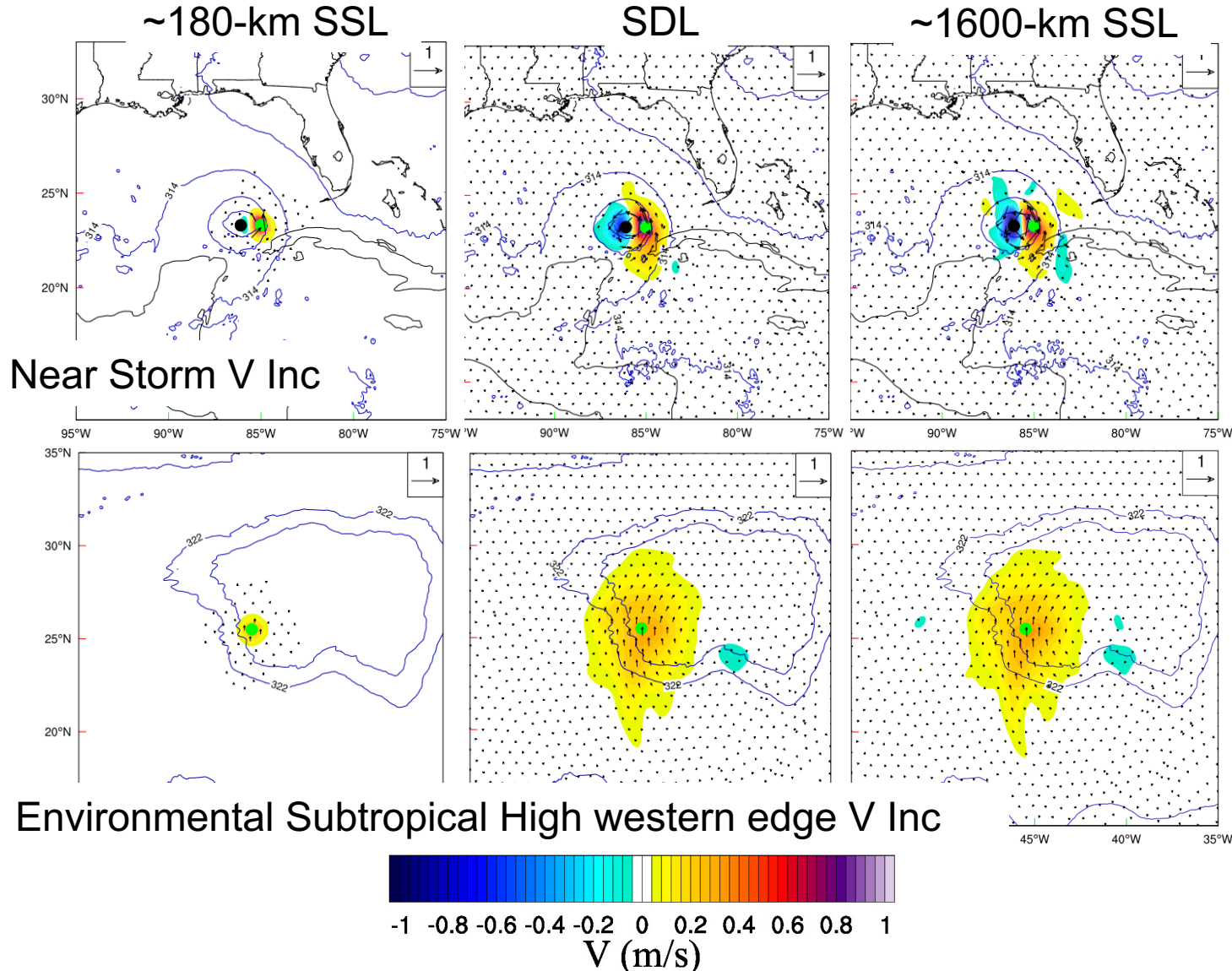




# Simultaneous MDA with SDL in HAFS 4DEnVar



Lu\* and Wang 2023a

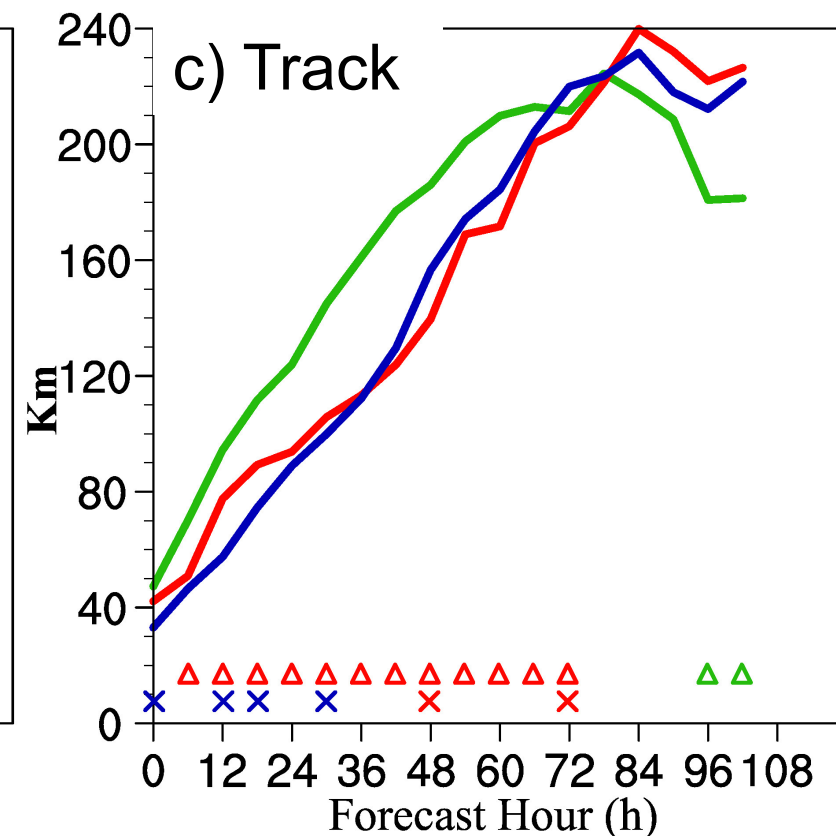
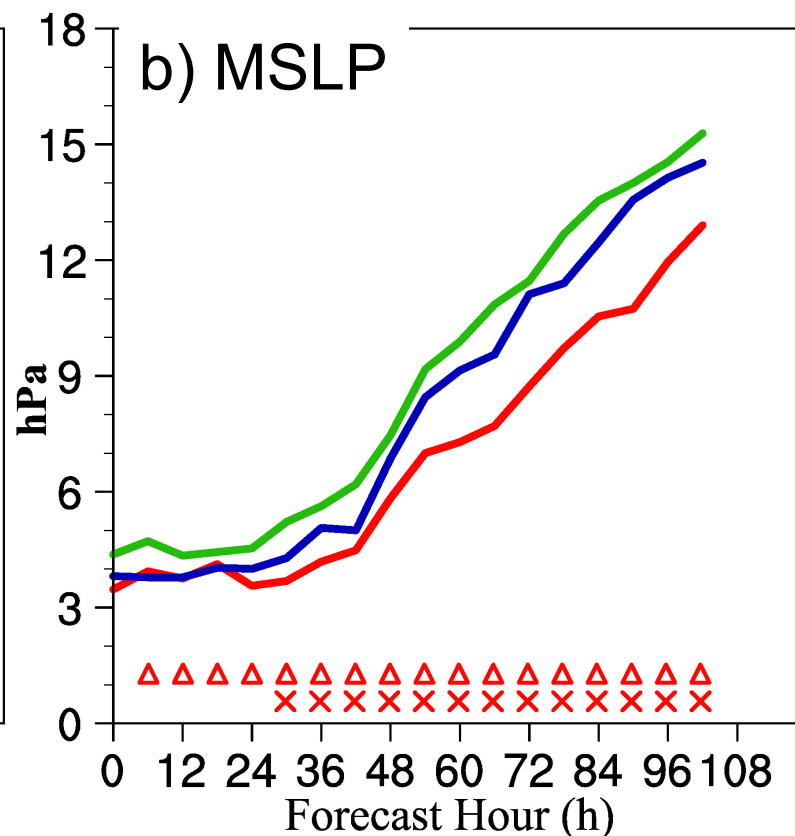
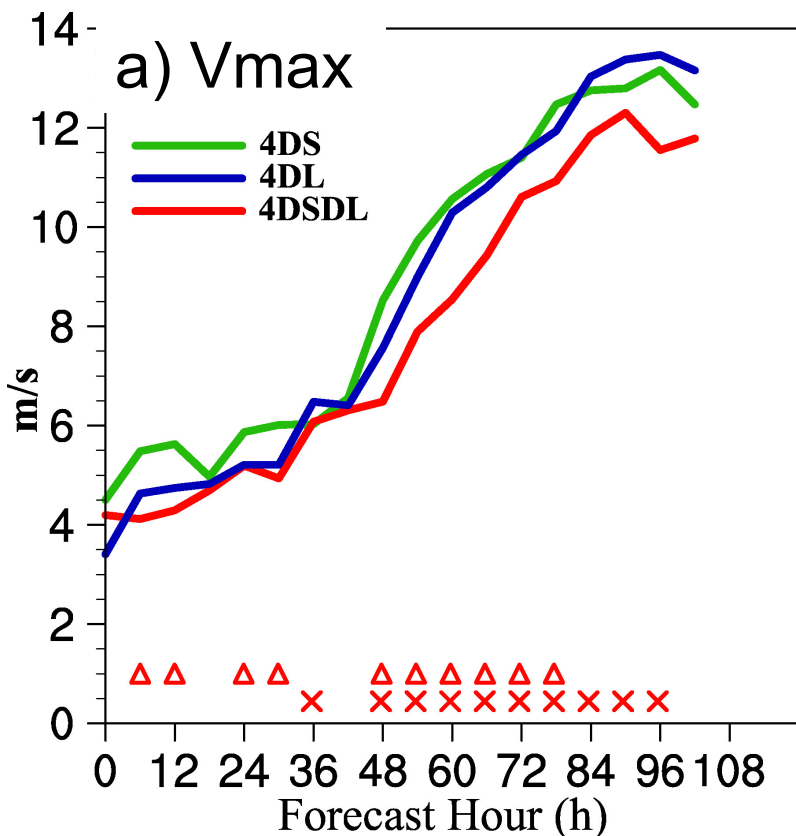


- The simultaneous MDA with SDL is recently further extended and implemented for HAFS EnVar
- MDA with SDL can simultaneously properly correct both the TC and its large scale steering environment (subtropical high)



# Impact on convection allowing hurricane forecasts

## Mean Absolute Forecast Errors during Hurricane Laura (2020)



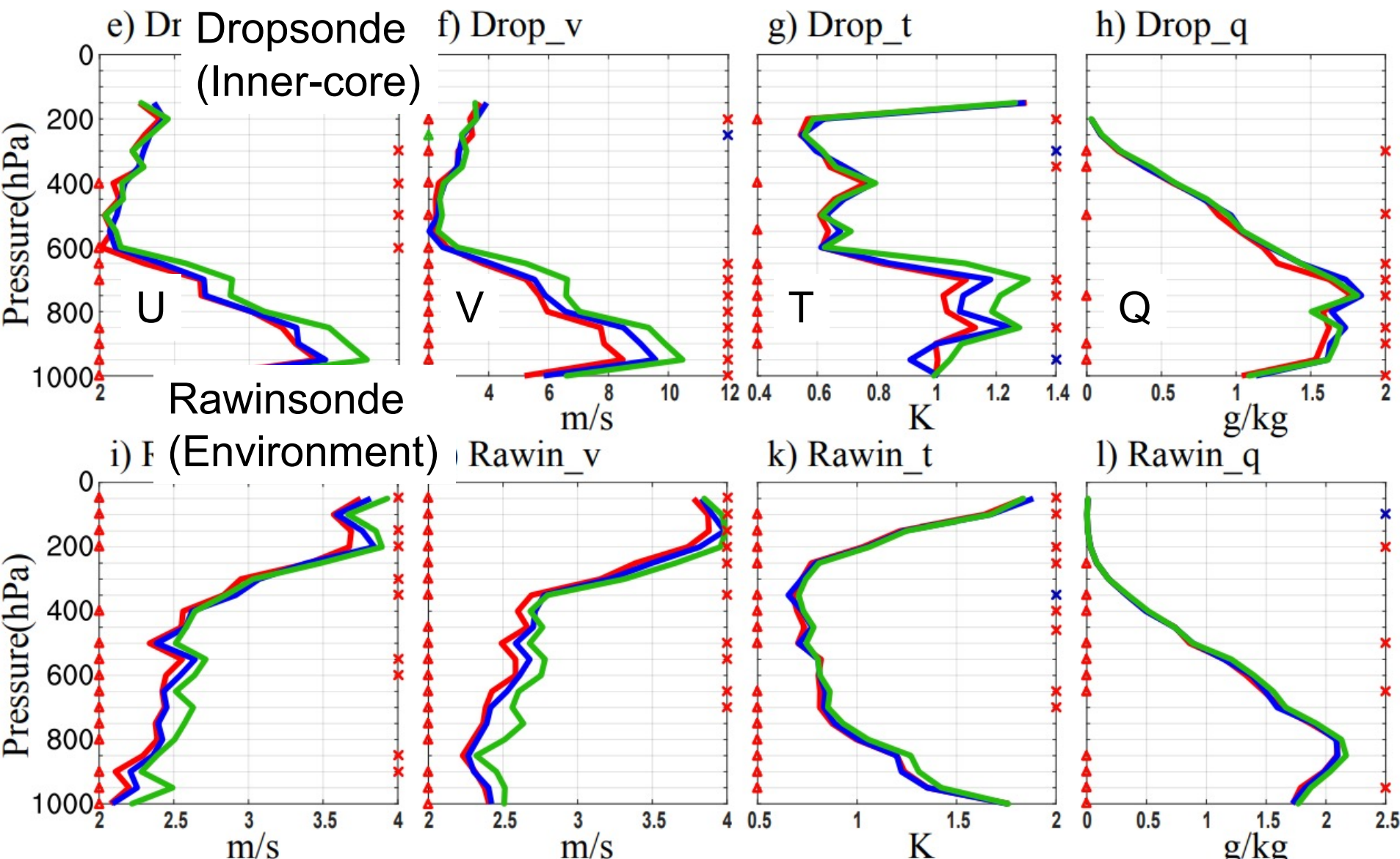
### ➤ Localization Impacts on Forecasts

- 4DSDL outperforms 4DL and 4DS in intensity predictions
- 4DSDL outperforms 4DS in track prediction and has mixed results compared to 4DL



# Impact of Simultaneous Multiscale DA

## 6-h Background Forecast Verification against Dropsonde & Rawinsonde



— 4DS  
— 4DL  
— 4DSDL

➤ MDA produces better background than SSL in both vortex scale and TC environment.



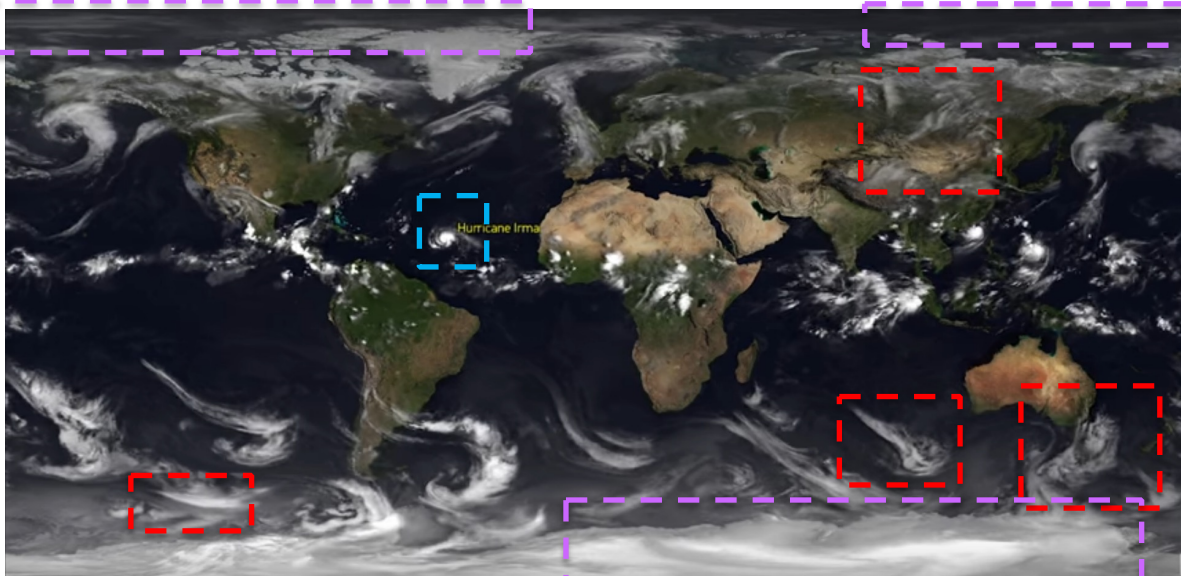
# Part III: Simultaneous MDA with flow dependent vertical localization (vFDL) for GFS 4DEnVar

Jone\* and Wang 2023b

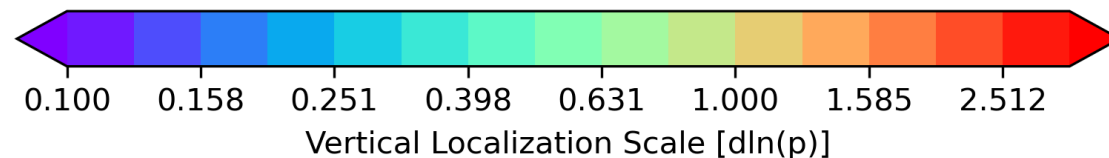
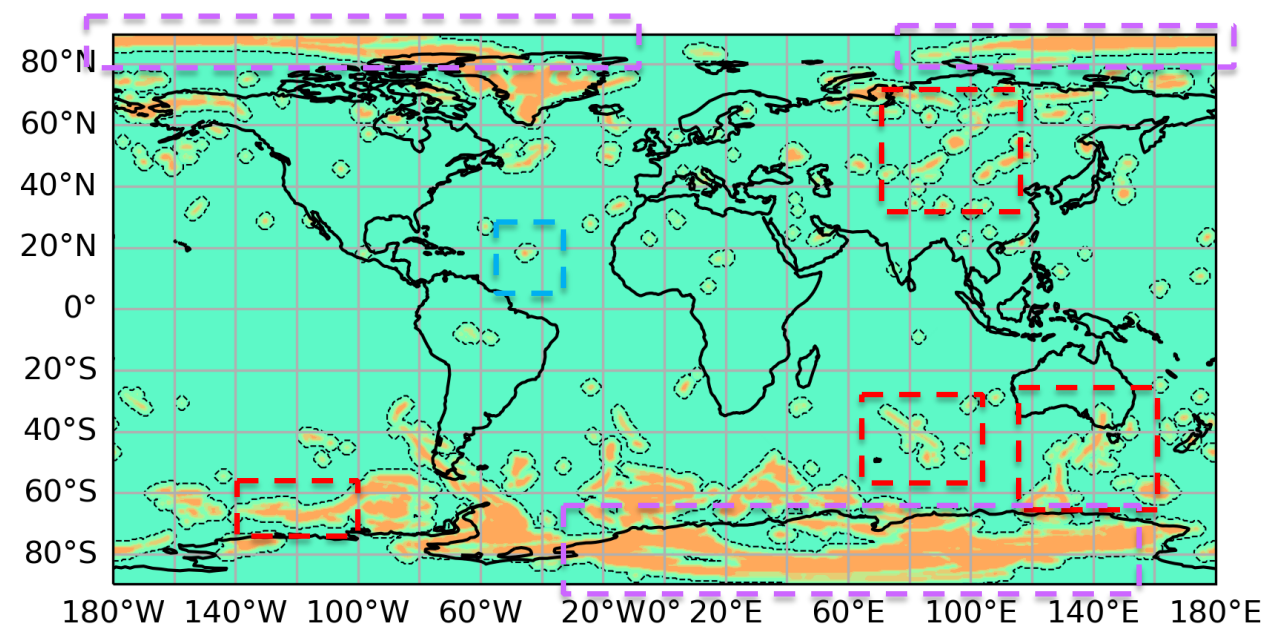


□ Areas identified for larger vertical localization lengths tend to be within:

- Tropical cyclones
- Frontal regions
- Broad polar regions



Courtesy of EUMETSAT



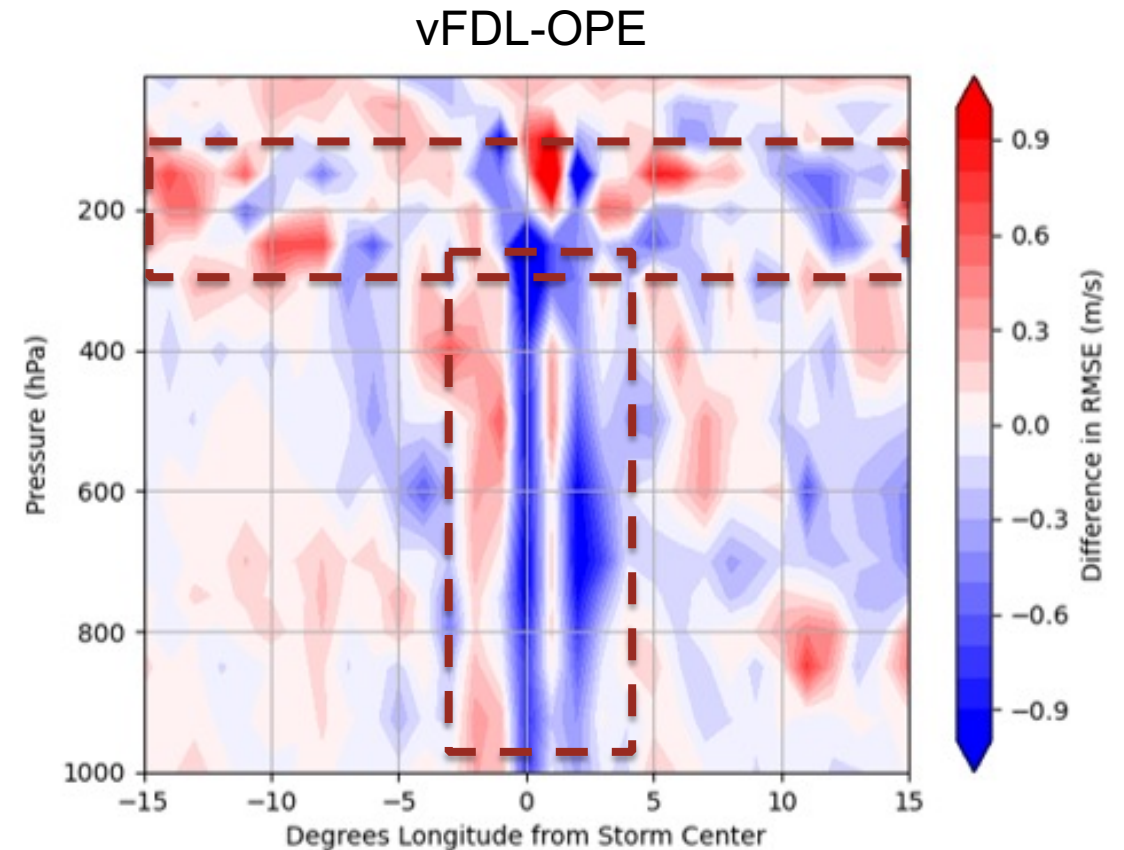
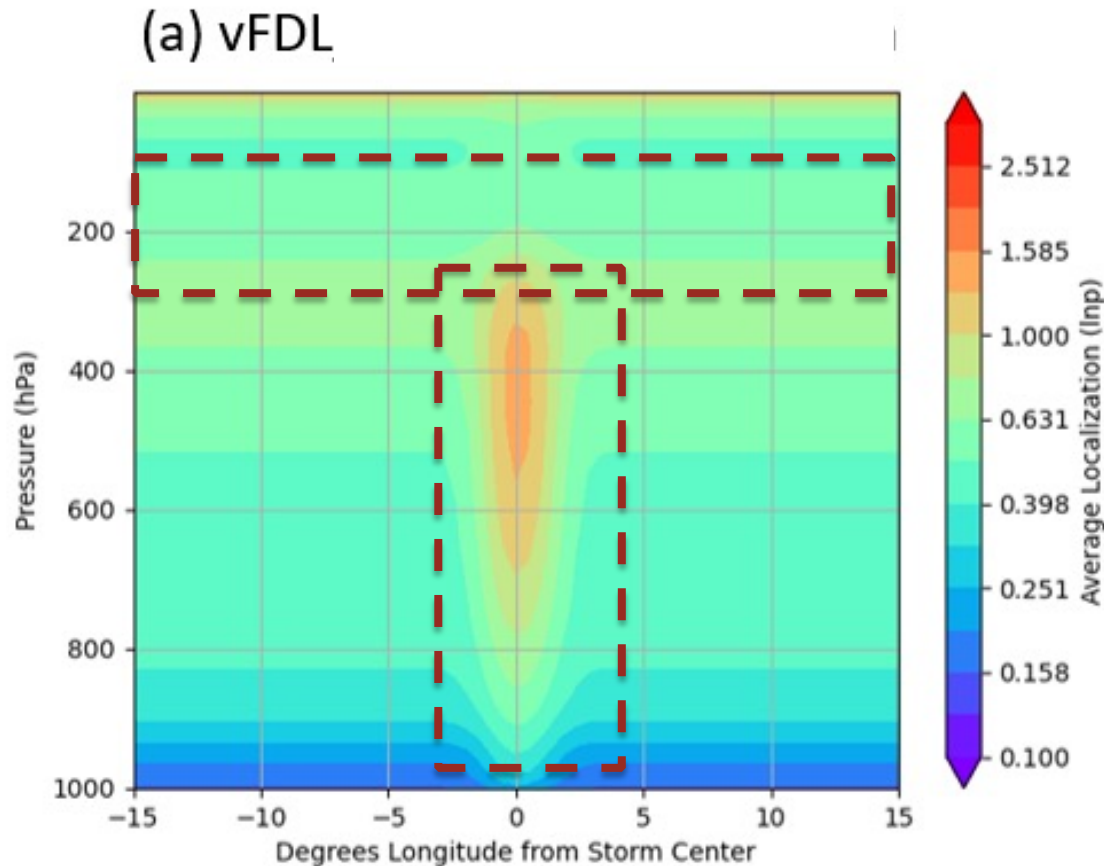


# Hurricane Irma (2017) Composite Localization and Difference in RMSE Cross Sections



Largest differences in RMSE tend to occur at ~200 hPa and in inner core at all levels

(b) Difference in V-wind RMSE

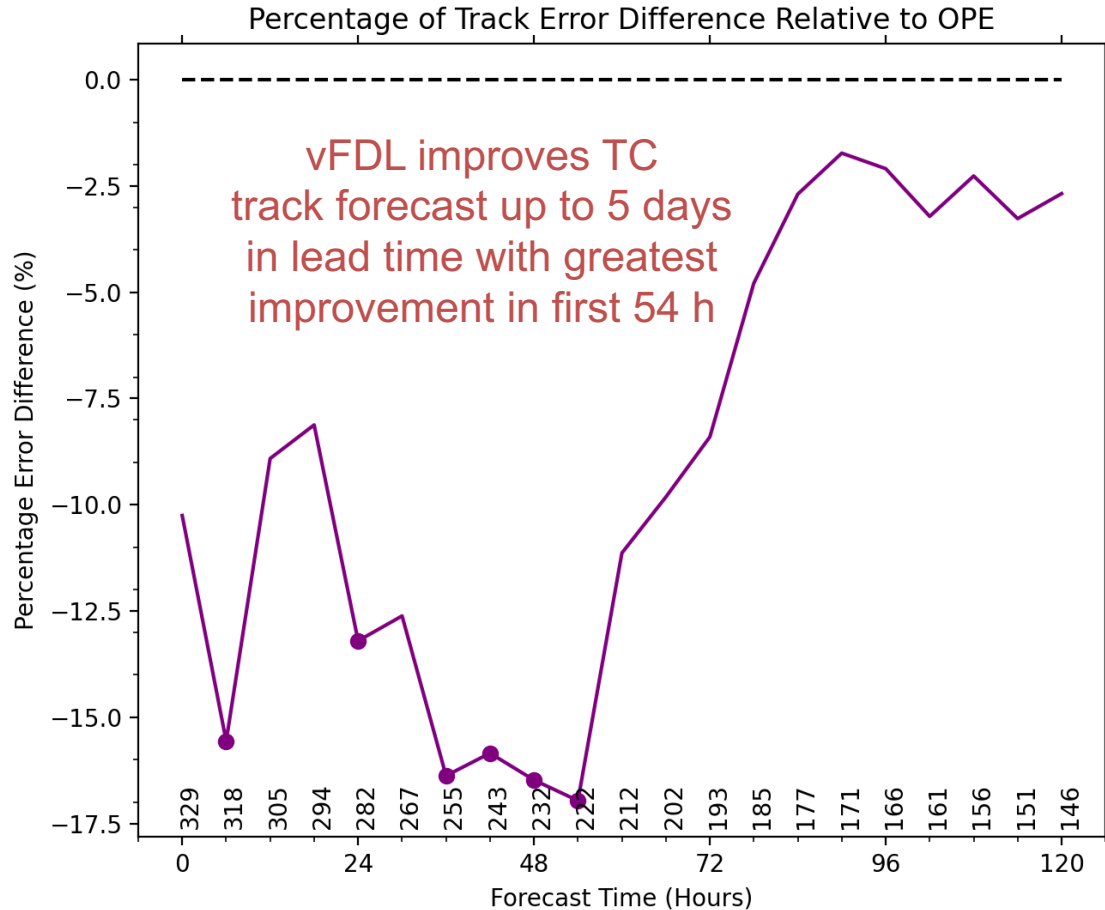


Most impact regions correspond with areas Identified for increased vertical localization





# Impact on month long GFS hurricane track forecasts



- Flow-dependent vertical localization show promises to improve GFS hurricane track forecasts
- Improved initial position leads to improved forecasts for the first 72 h
- Large scale improvement in zonal wind leads to improvement after 72 h

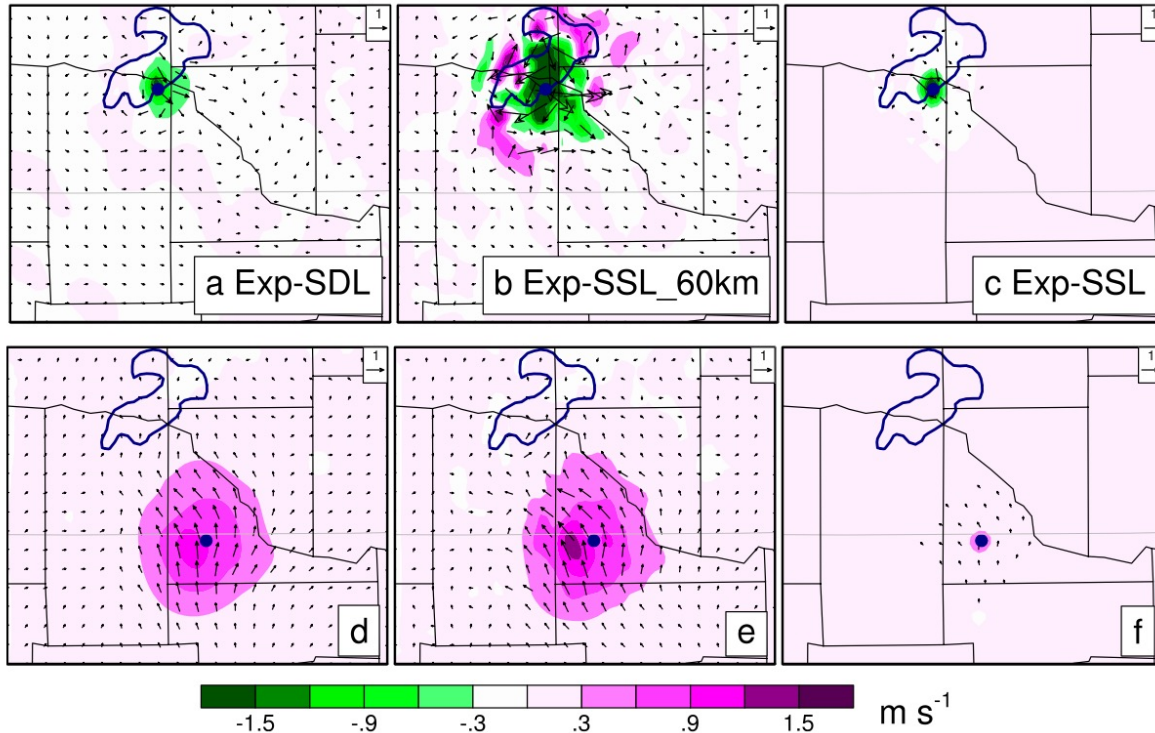
Tracking algorithm by Marchok (2002). Numbers above the x-axis denote how many tracks at each lead time. Filled dots indicate 95% confidence using a paired *t*-test.



# Part IV: Simultaneous MDA with scale and variable dependent localization (SDLVLD) for WoF & HRRR/RRFS EnVar



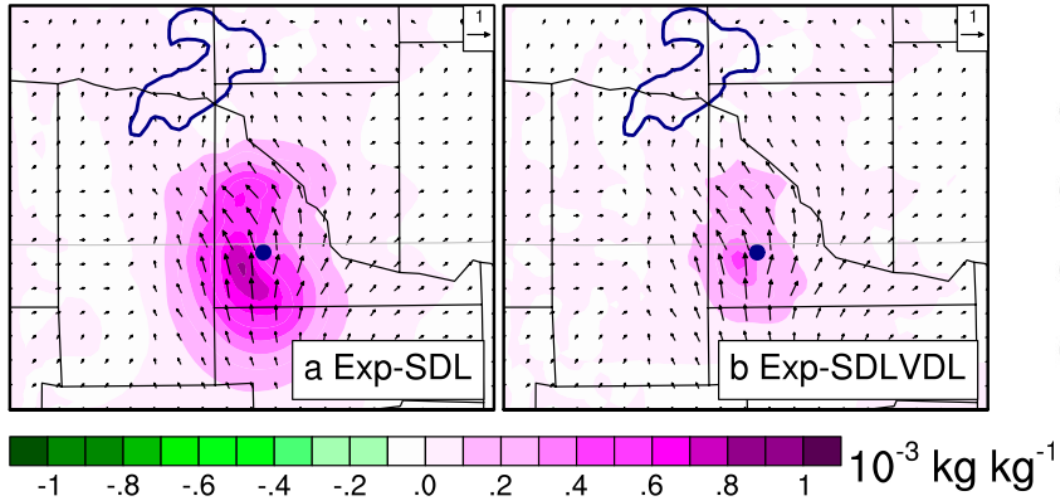
Wang\* and Wang 2023ab



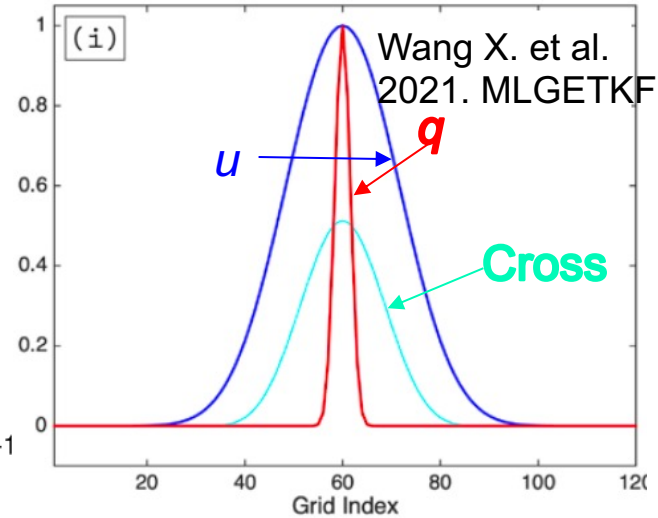
Wang, Y.\* and X. Wang 2023a

- MDA with SDL can simultaneously properly correct both the supercell storm and its ambient environment, which represent different scales

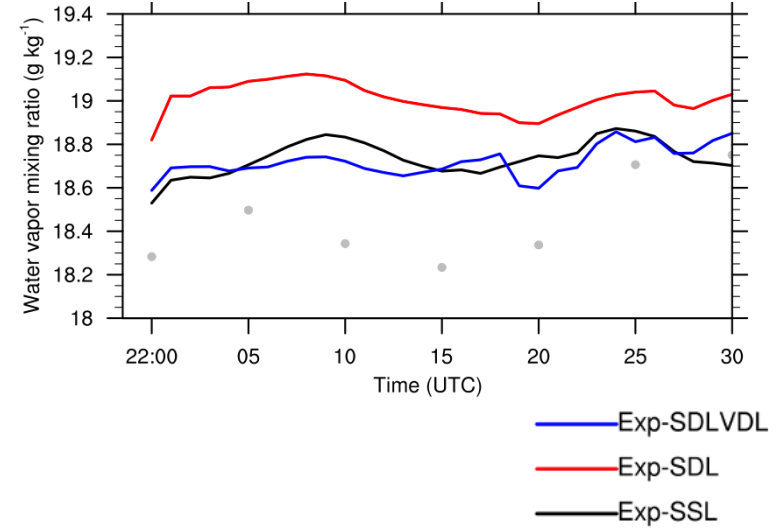
Analysis increments of wind (vector) and v-wind (shaded) through assimilating a single observation of  $V_r$  with an innovation of  $-30 \text{ m/s}$  at  $1 \text{ km AGL}$ .



localization function



Overestimated q in Exp-SDL



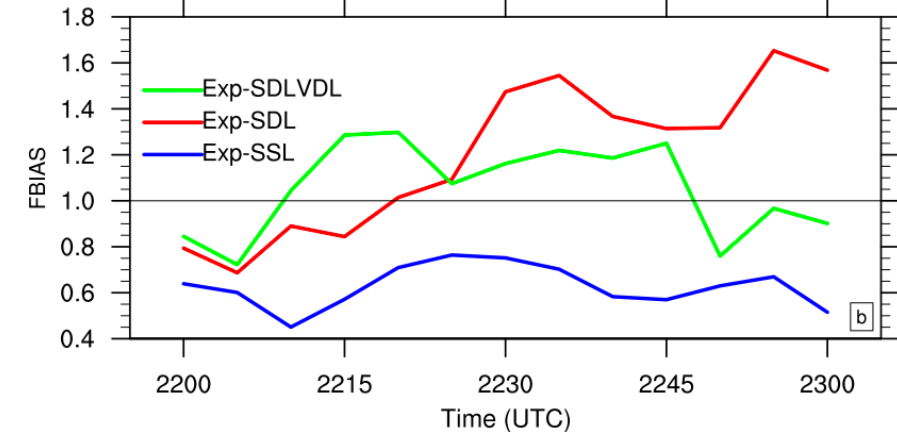
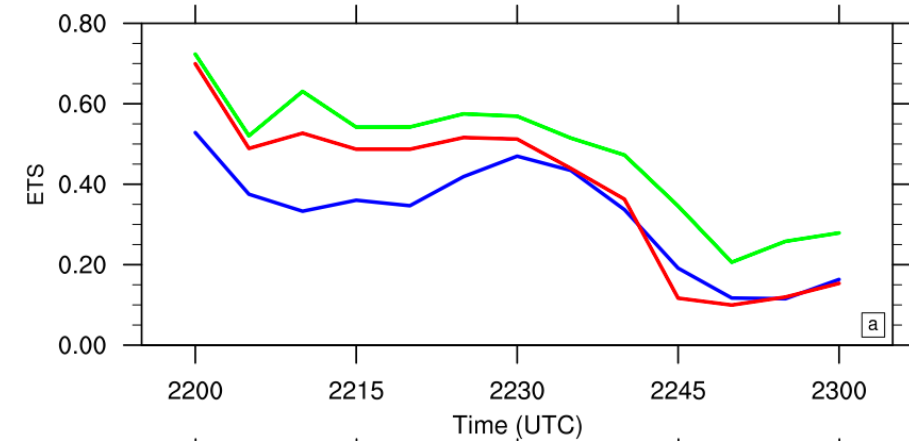
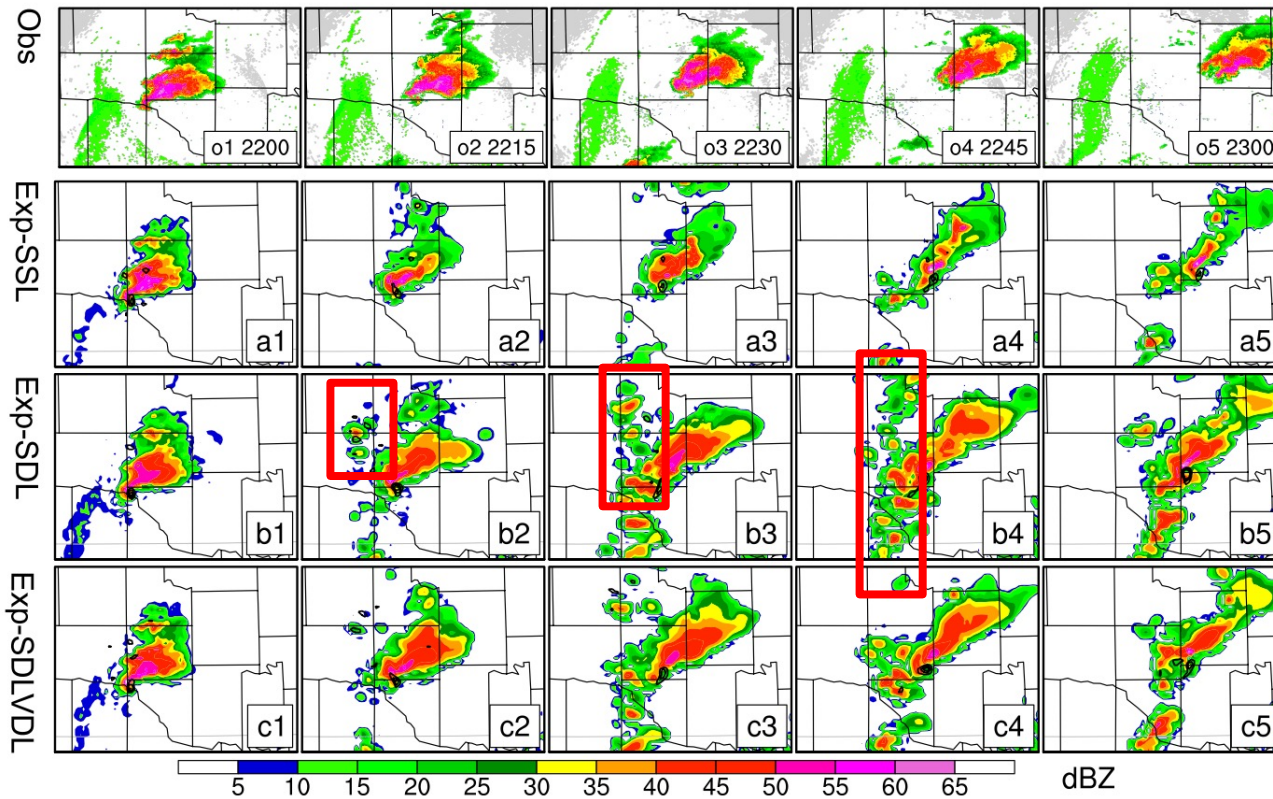
SDLVDL (Wang, Y\* and. X. Wang 2023a)

$$\hat{\mathbf{L}}_{m,n} = \begin{bmatrix} \hat{\mathbf{L}}_{m_1,n_1} & \hat{\mathbf{L}}_{m_1,n_2} & \cdots & \hat{\mathbf{L}}_{m_1,n_Y} \\ \hat{\mathbf{L}}_{m_2,n_1} & \hat{\mathbf{L}}_{m_2,n_2} & \cdots & \hat{\mathbf{L}}_{m_2,n_Y} \\ \vdots & \vdots & \ddots & \vdots \\ \hat{\mathbf{L}}_{m_Y,n_1} & \hat{\mathbf{L}}_{m_Y,n_2} & \cdots & \hat{\mathbf{L}}_{m_Y,n_Y} \end{bmatrix},$$

- Using VDL with an appropriately smaller localization for q greatly reduces intensity and coverage of moisture increments compared to using SDL only.



# Impact on supercell forecasts (Reflectivity @ 1km AGL)



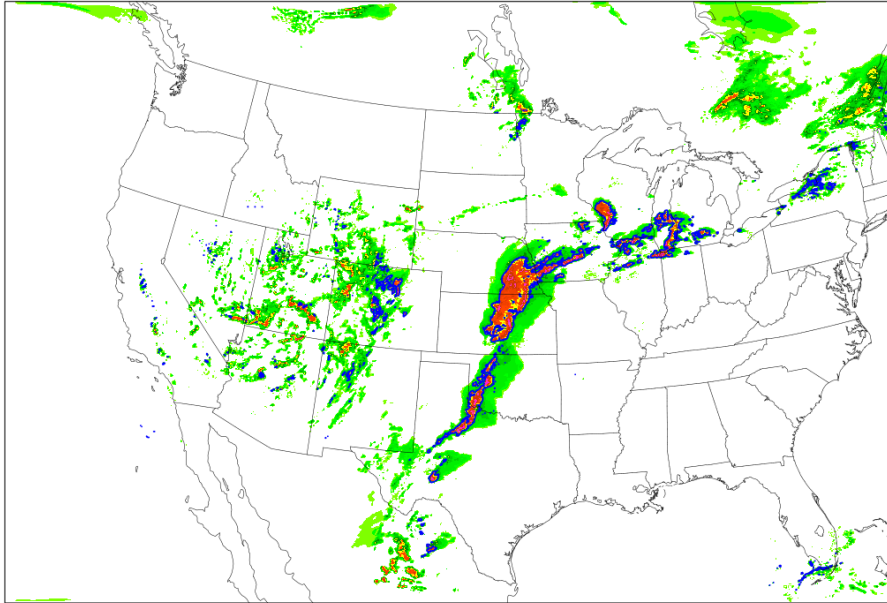
- Compared to Exp-SSL, Exp-SDL and Exp-SDLVDL improve the forecasts for the forward-flank distributions;
- Exp-SDLVDL has less spurious storms and further enhances supercell than Exp-SDL



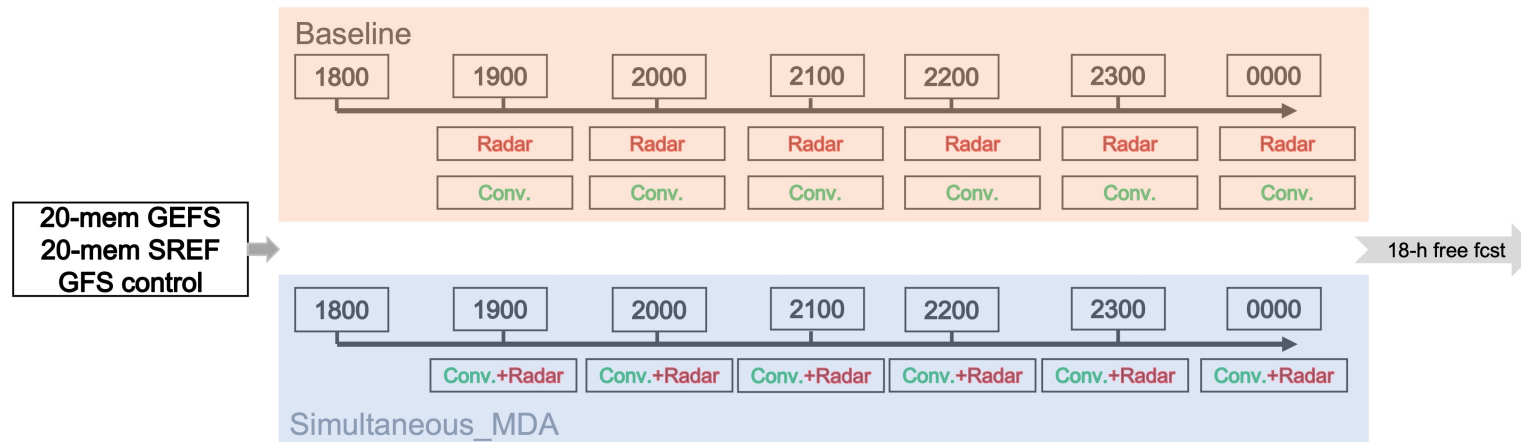
# Experiment design (HRRR/RRFS)

## Model and DA configuration

Wang, Y.\* and X. Wang 2023b



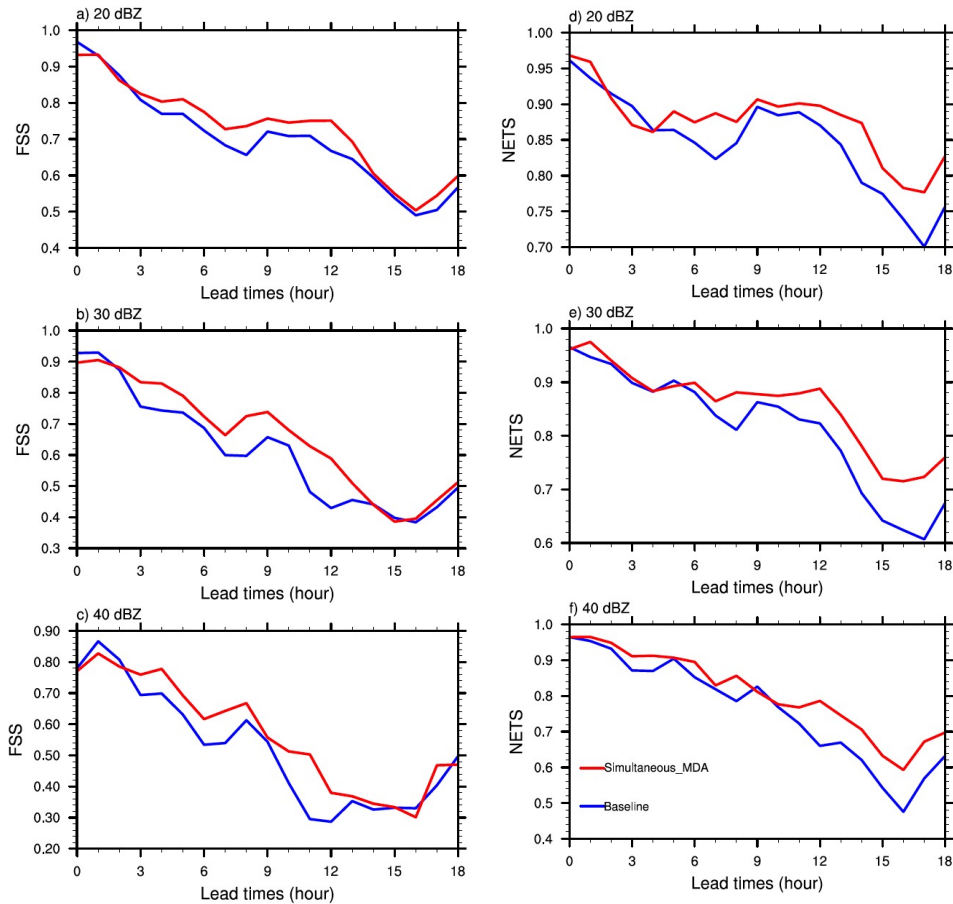
Model options	Specification
Grid size and resolution	1621×1121×51; 3 km
Microphysics	Thompson
PBL	MYNN
Radiation	RRTMG
Land surface model	Noah





# Impacts of SDLVDL in EnVar on RRFSS/HRRR forecasts

Wang Y.\* and X. Wang 2023b



➤ For composite reflectivity forecast, Simultaneous\_MDA outperforms Baseline in the majority of forecast leading time.

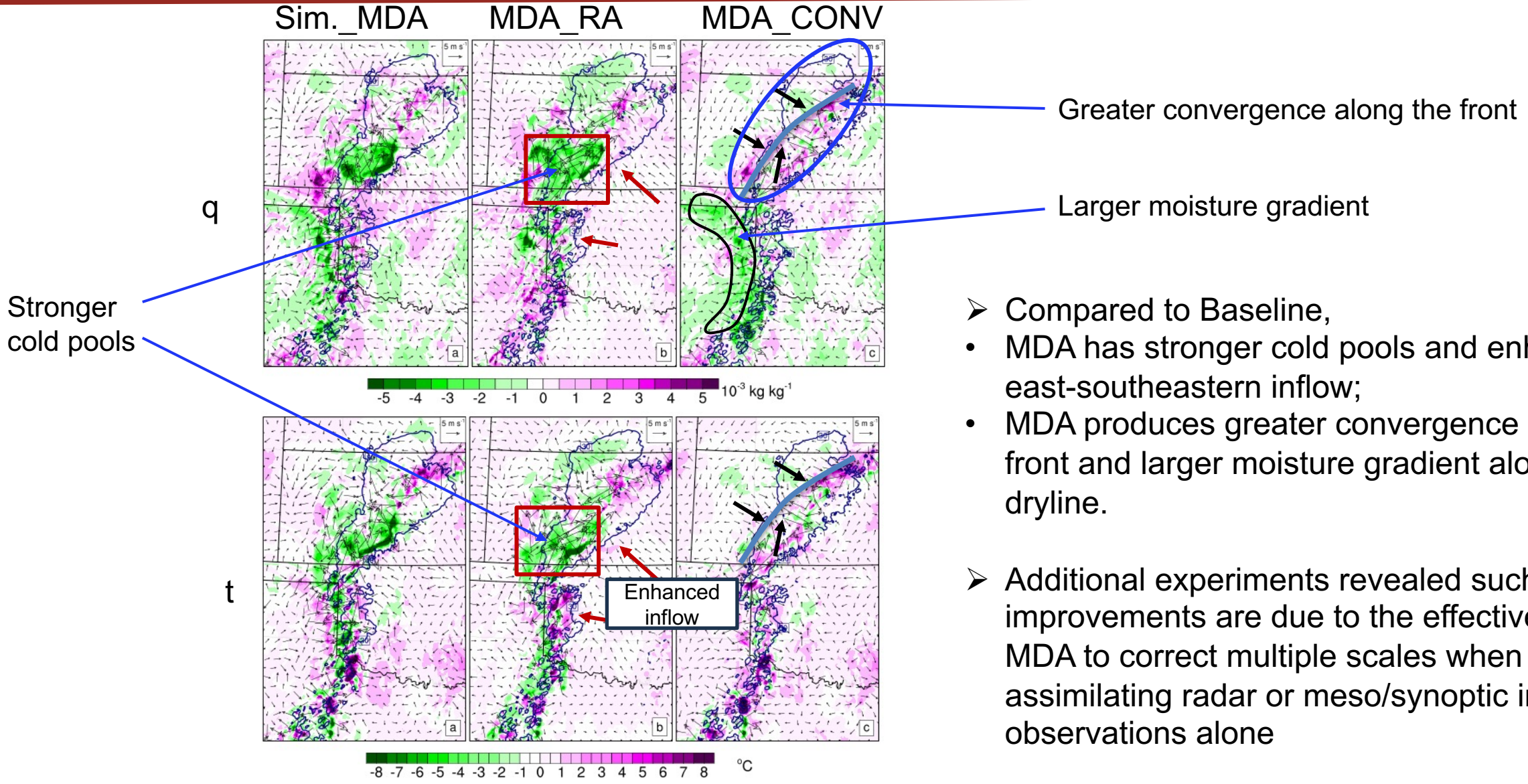
FSS and NETS for composite reflectivity



# Understanding the impact of Simultaneous\_MDA on RRFS/HRRR forecast



Analysis differences with Baseline



- Compared to Baseline,
  - MDA has stronger cold pools and enhanced east-southeastern inflow;
  - MDA produces greater convergence along the front and larger moisture gradient along the dryline.
- Additional experiments revealed such improvements are due to the effectiveness of MDA to correct multiple scales when assimilating radar or meso/synoptic in-situ observations alone

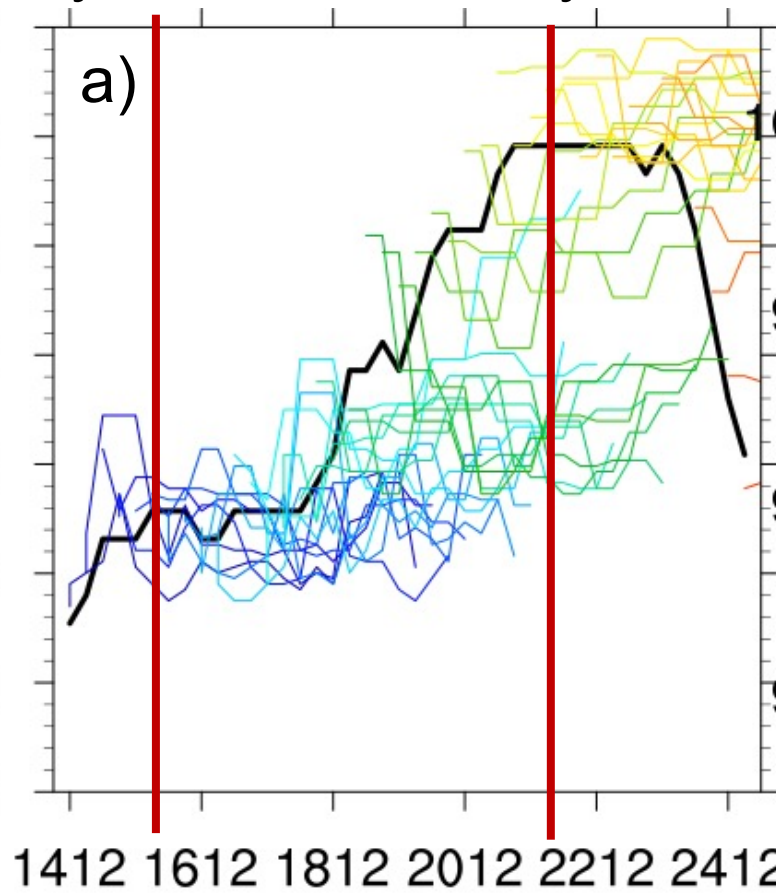


# Part V: coupled ocean-atm DA for TC

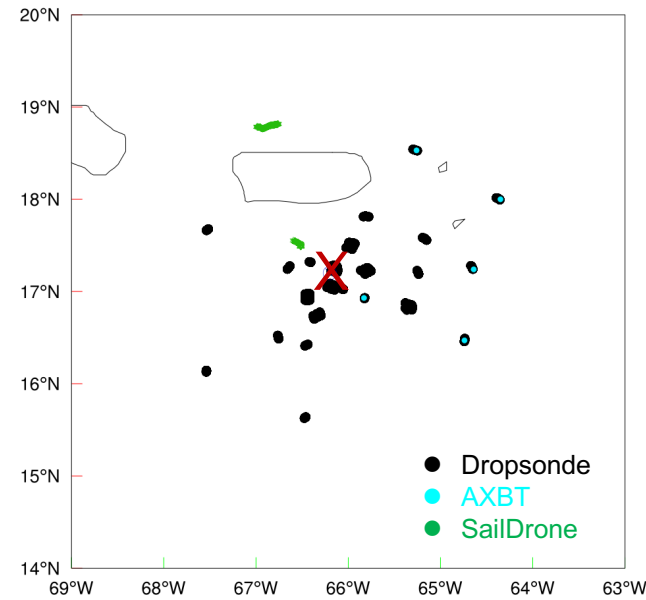


Lu\* and Wang et al. 2023b

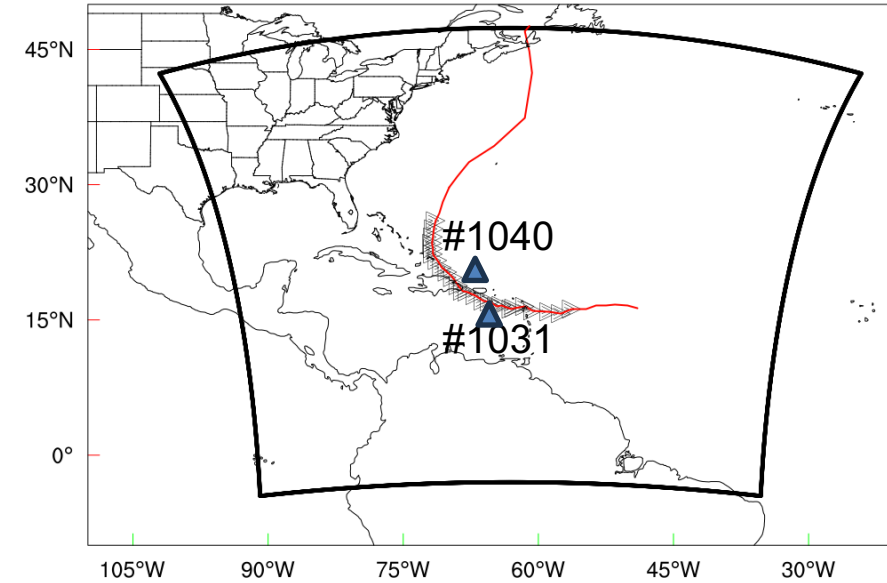
Cycle Starts      Cycle Ends



b)



c)



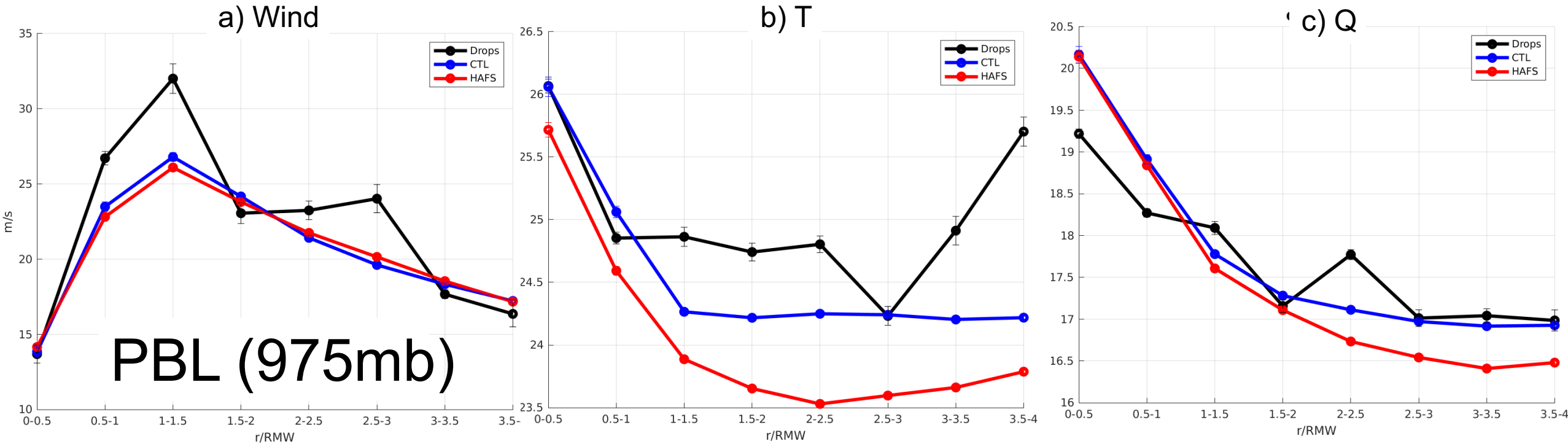
Finoa 2022





# Model Performance Verification

## Azimuthal Verifications of PBL Structures from Dropsondes



- CTL experiment matches the dropsonde observations reasonably well.
- CTL performs even slightly better than the HAFS-A operational run in 2022.

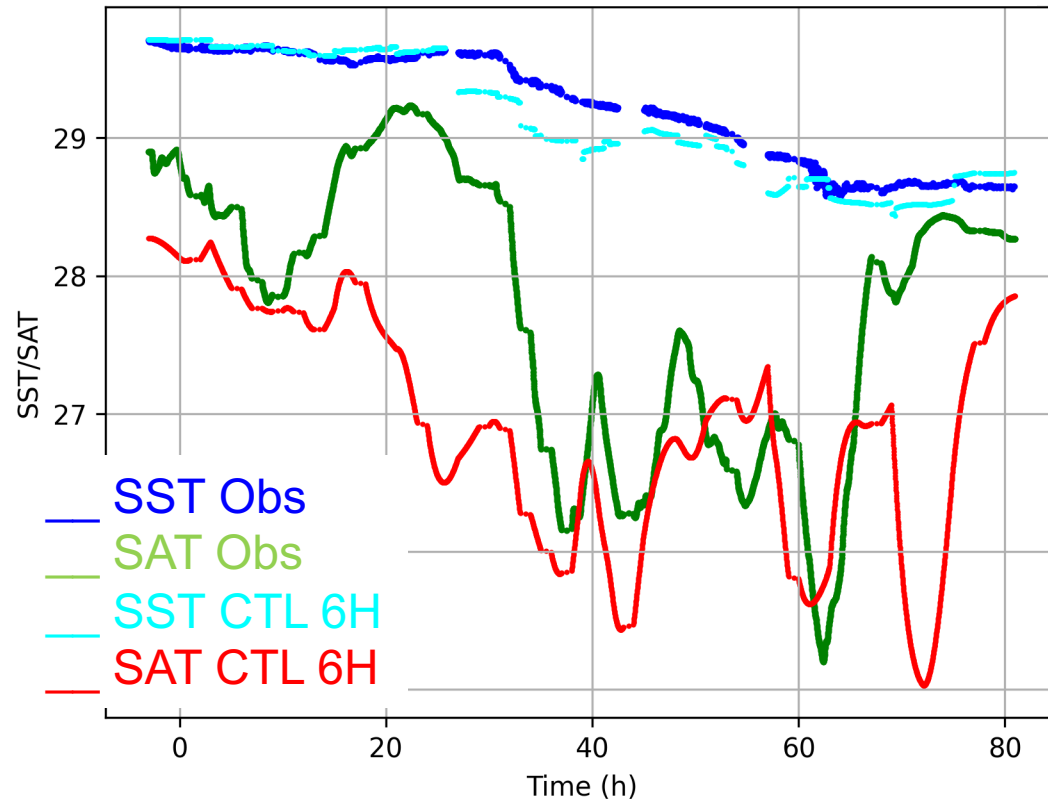


# Model Performance Verification

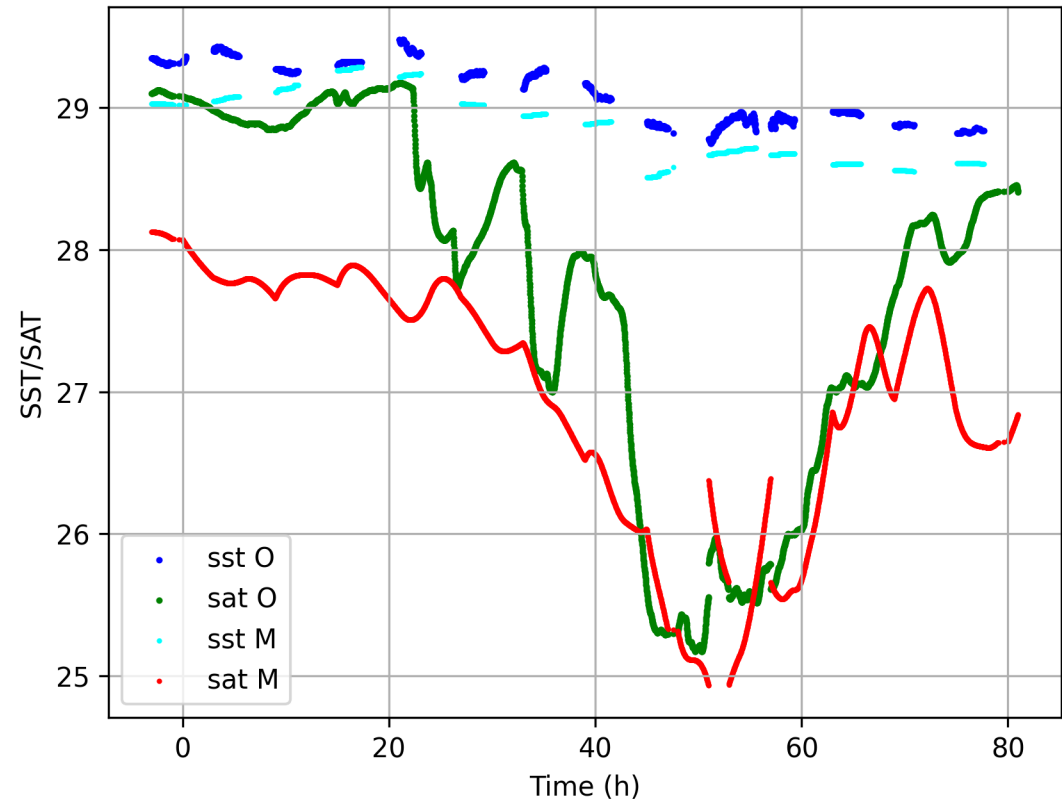
## Air-Sea Interface verifications from SailDrones



a) Saildrone #1031 (smoothed)



b) Saildrone #1040 (smoothed)

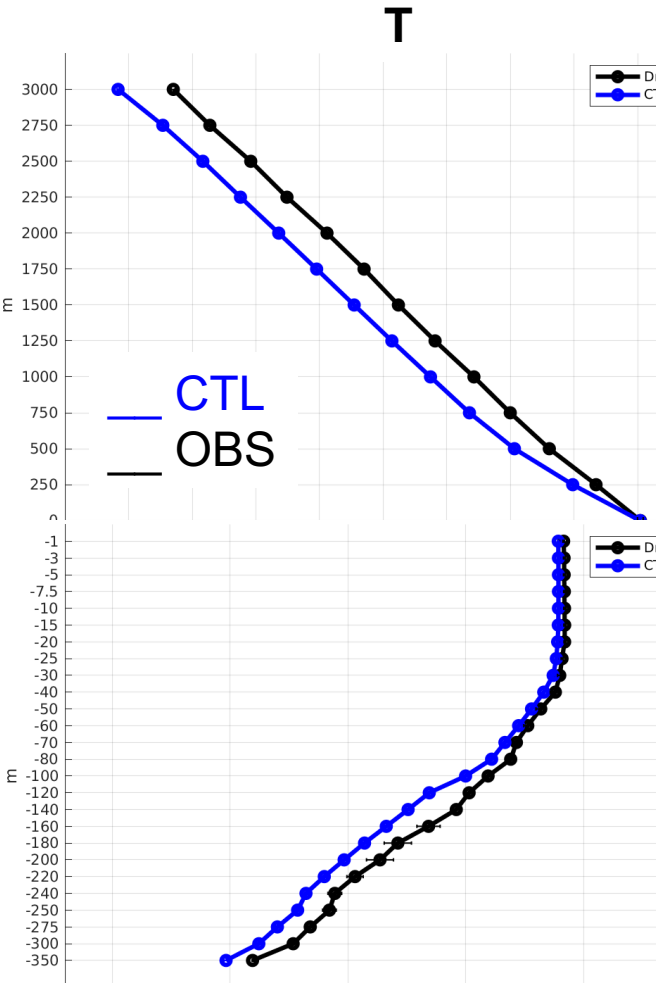


✓ Low bias in both SAT and SST from the model

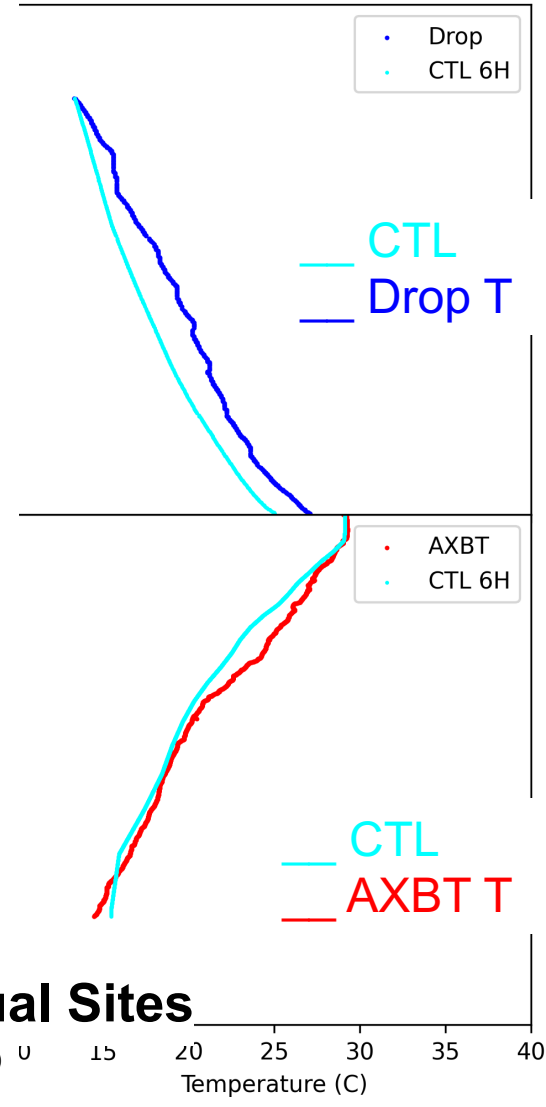
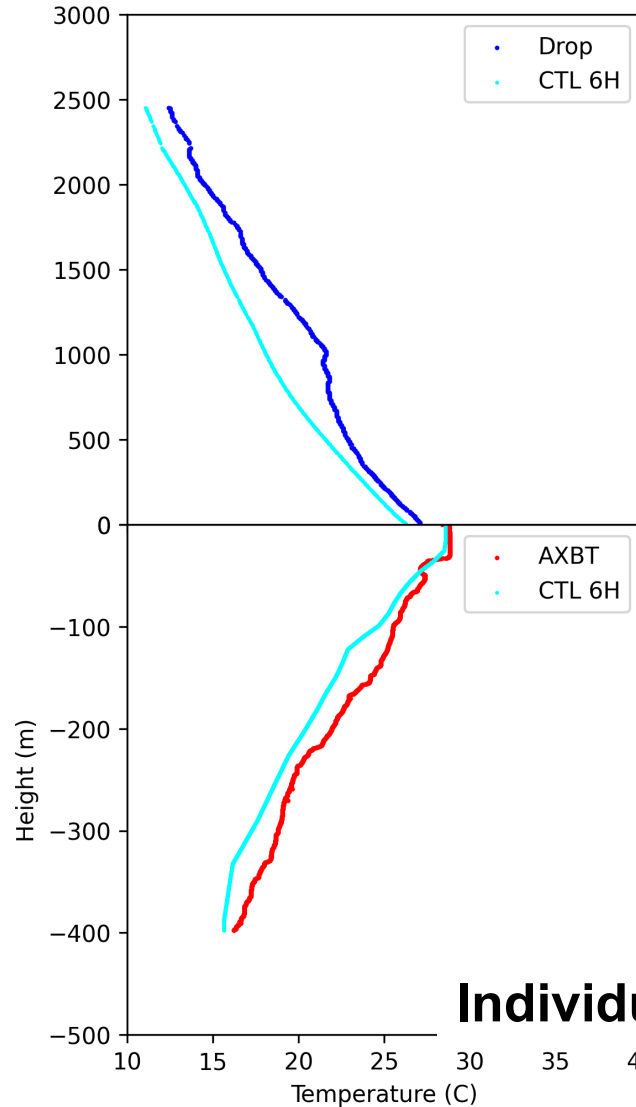


# Model Performance Verification

## Air-Sea Interface verifications from Drops + AXBT



**Avg @ 1.75-2.25 RMW**



✓ Slight negative model biases still exists in both air and sea.



# Part VI: MLGETKF and Scale Dependent Inflation



Wang, X. et al., 2021, Xu\* et al, 2023

- ❑ A new ensemble-based, multiscale data assimilation (MDA) method, MLGETKF (Multiscale Local Gain Form Ensemble Transform Kalman Filter, Wang et al. 2021), was developed.

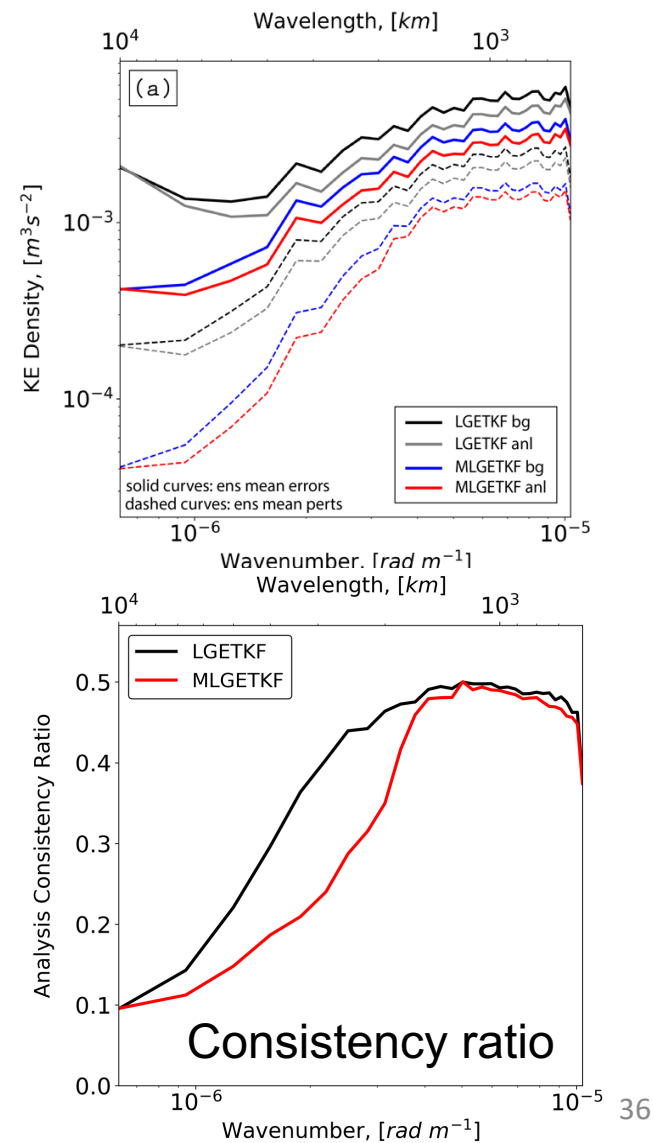
$$\mathbf{z}^{ML} = (\mathbf{z}_1, \mathbf{z}_2, \dots, \mathbf{z}_{K_{ML}}) = (\mathbf{I} \quad \mathbf{I} \quad \dots \quad \mathbf{I}) \left( \mathbf{X}^{MS} \Delta \left[ \left( \mathbf{L}^{MS} \right)^{\frac{1}{2}} \right] \right)$$

Modulated/expanded pseudo ensemble perturbations

Scale decomposed raw perturbations

Multiscale model space localization

- ❑ MLGETKF reduces analysis and background errors relative to scale unaware LGETKF for all scales, especially towards the large scales.
- ❑ The same study also reveals that the common issue of background ensemble under-sampling can be scale dependent





# Methodology

## Scale dependent RTPS inflation (RTPS-SDI)

Naicheng Xu Thur. poster



□ The RTPS inflation (Whitaker and Hamill 2012) relaxes the posterior spread toward the prior spread

- Inflation factor  $\mathbf{g} = \alpha * \frac{\sqrt{\mathbf{P}^b} - \sqrt{\mathbf{P}^a}}{\sqrt{\mathbf{P}^a}} + 1$

□ In this study, RTPS is further developed and implemented separately for different scales (hereafter “RTPS-SDI”)

- Inflation factor  $\mathbf{g}_m = \alpha_m * \frac{\sqrt{\mathbf{P}_m^b} - \sqrt{\mathbf{P}_m^a}}{\sqrt{\mathbf{P}_m^a}} + 1$



# Methodology

## Scale dependent inflation based on sampling error (SE-SDI)



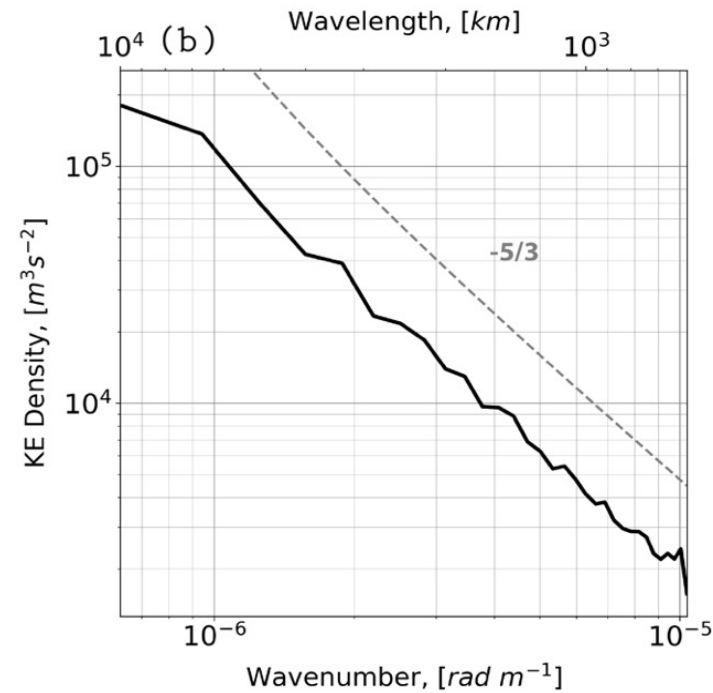
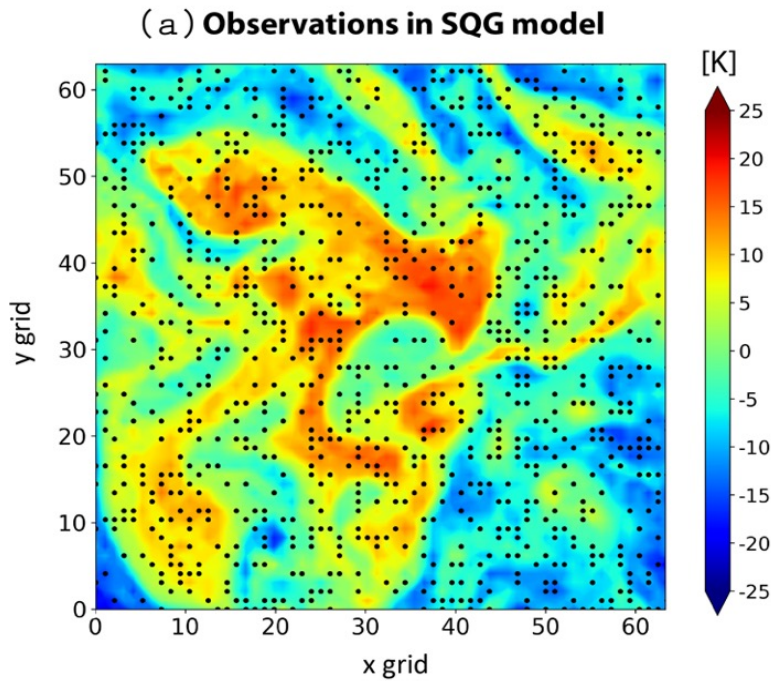
- Hodyss et al. (2016), using the ensemble Kalman filter theory, derived a posterior inflation that accounts for the sampling error deficiency (hereafter “SE” inflation)

- $\mathbf{S} \approx a * \mathbf{P}^a + \left( \frac{\mathbf{P}^a}{\mathbf{P}^b} \right)^2 \left( b \frac{\mathbf{P}^b}{N_e} + c \frac{2}{N_e - 1} (\bar{\mathbf{x}}^a - \bar{\mathbf{x}}^b)^2 \right)$  Inflation factor:  $\mathbf{g} = \sqrt{\frac{\mathbf{S}}{\mathbf{P}^a}}$

Additional analysis error due to limited ensemble members, i.e., sampling error

- Scale dependent SE inflation (hereafter “SE –SDI” inflation):
- Starting with the multiscale analysis equation (equivalent to MLGETKF if assuming no cross scale covariance), rederive SE inflation for different scales of analysis

- $\mathbf{S}_m \approx a_m \mathbf{P}_m^a + \left[ \left( \frac{\mathbf{P}_m^a}{\mathbf{P}_m^b} \right)^2 \left( b_m \frac{\mathbf{P}_m^b}{N_e} + c_m \frac{2}{N_e - 1} (\bar{\mathbf{x}}_m^a - \bar{\mathbf{x}}_m^b)^2 \right) \right]$  Inflation factors:  $\mathbf{g}_m = \sqrt{\frac{\mathbf{S}_m}{\mathbf{P}_m^a}}$



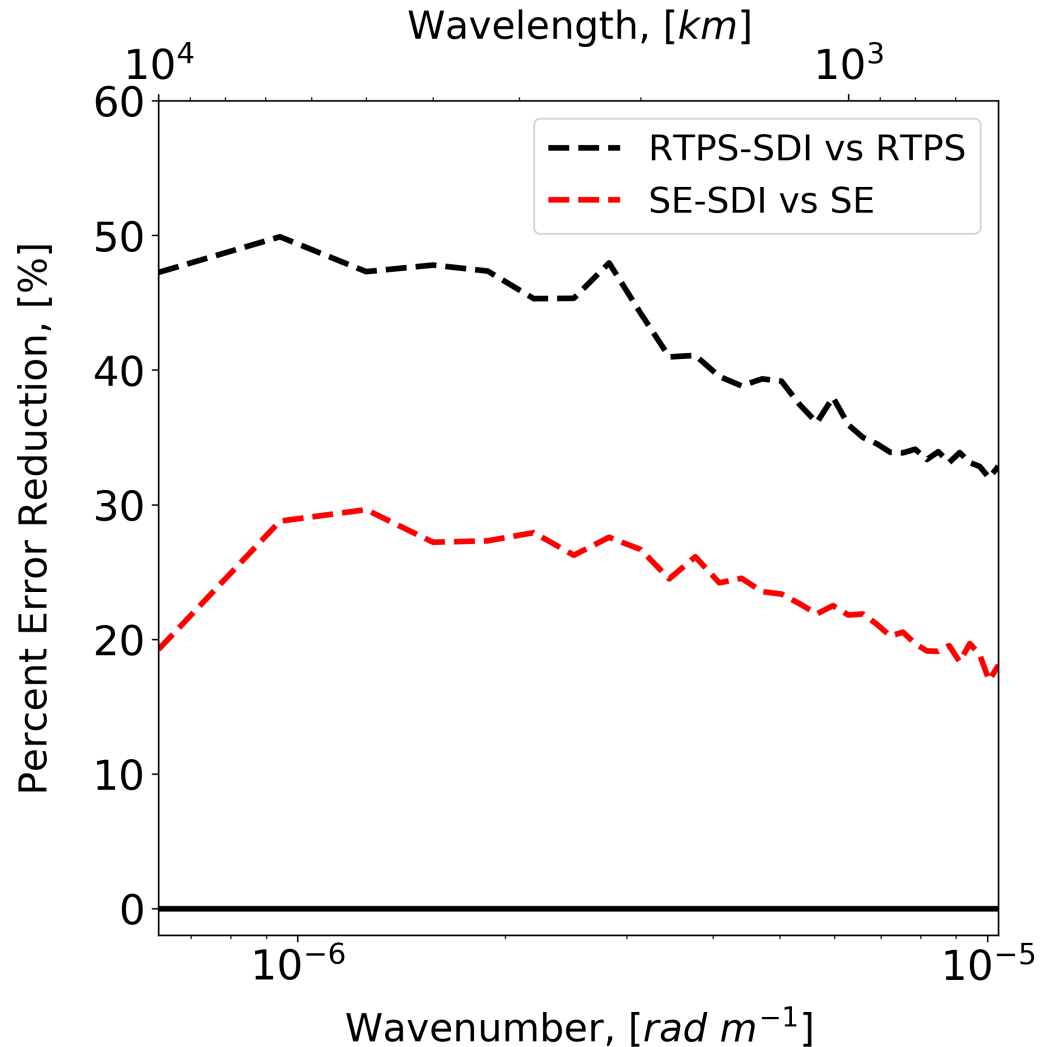
- SQG turbulence model follows Tulloch and Smith (2009) and mimics mesoscale of the atmosphere
- The four inflation methods are implemented on MLGETKF (Wang X. et al. 2021)
- Simulated obs.: potential temperature on both model surfaces with a standard deviation of 1K
- Ensemble size: 20-member
- 3-hourly data assimilation is performed for 400 cycles

Exp. Name	Description
RTPS	Use RTPS for MLGETKF posterior inflation (Wang X. et al. 2021)
RTPS-SDI	Use scale dependent RTPS for MLGETKF posterior inflation
SE	Use sampling error (SE) derived inflation for MLGETKF posterior inflation
SE-SDI	Use scale dependent SE inflation for MLGETKF posterior inflation



# Development of scale dependent inflation (SDI) methods

Xu\* et al. 2023



- Both SDI methods show improved analysis accuracy across all resolved scales relative to their own scale independent inflation counter parts.

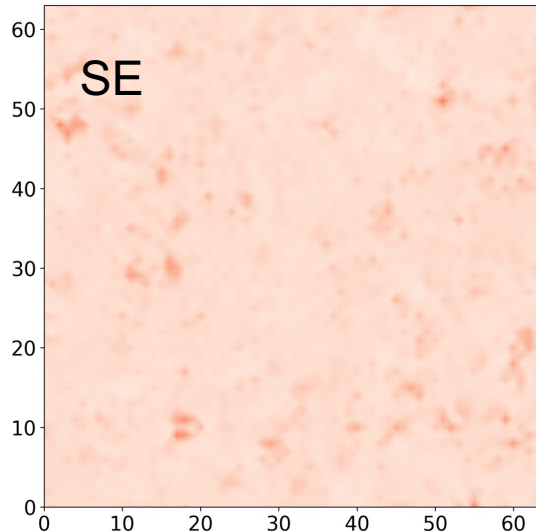




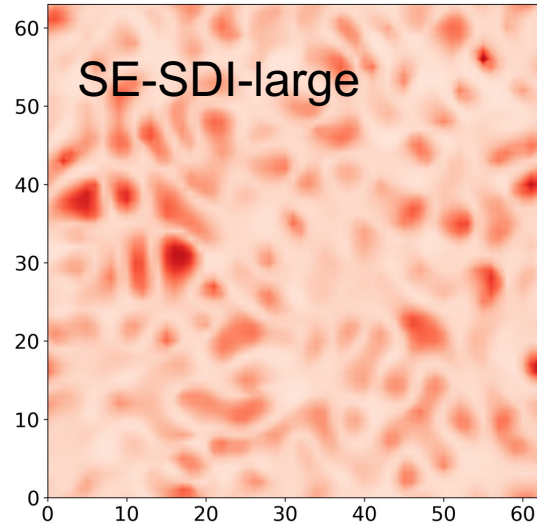
# Temporal and spatial behaviors of the inflation



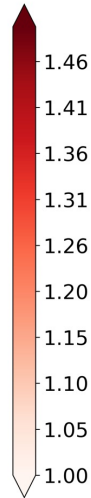
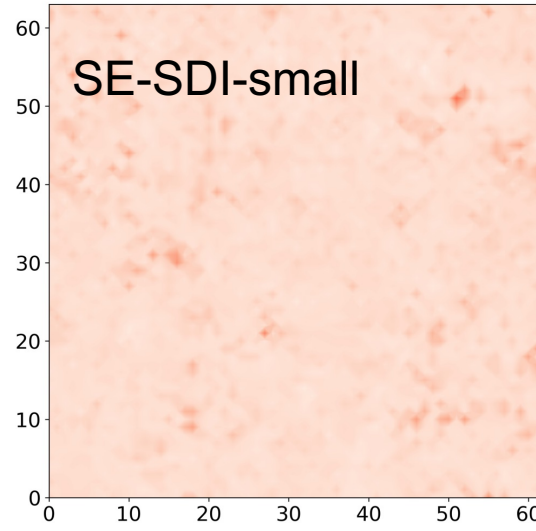
MLGETKF SE inflation (full) at  $z=2$  and  $t=200$   
min=1.03, mean=1.07, max=1.21



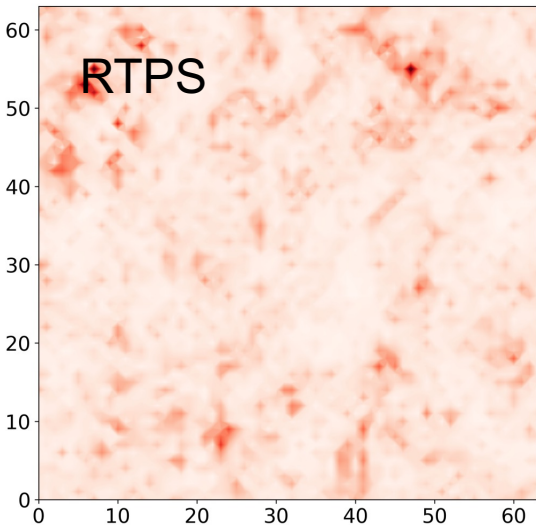
MLGETKF SE-SDI inflation (large) at  $z=2$  and  $t=200$   
min=1.05, mean=1.11, max=1.44



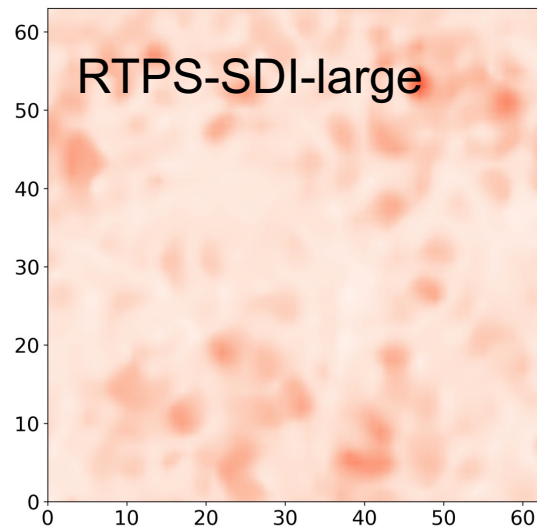
MLGETKF SE-SDI inflation (small) at  $z=2$  and  $t=200$   
min=1.02, mean=1.07, max=1.24



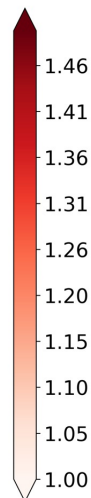
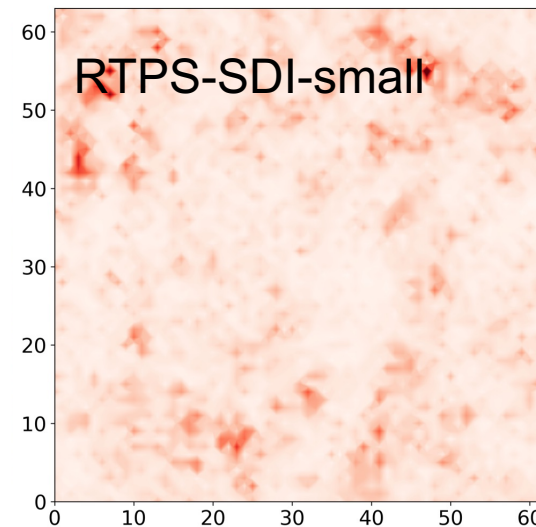
MLGETKF RTPS inflation (full) at  $z=2$  and  $t=200$   
min=1.00, mean=1.05, max=1.58



MLGETKF RTPS-SDI inflation (large) at  $z=2$  and  $t=200$   
min=1.01, mean=1.07, max=1.27



MLGETKF RTPS-SDI inflation (small) at  $z=2$  and  $t=200$   
min=0.99, mean=1.05, max=1.71



- In the two SDI experiments, the inflation factors at large and small scales reflect the corresponding scale structure.



# Summary and Remarks



- ❑ Great challenges exist to achieve effective multiscale DA for next generation NWP
  - Individual earth system component (e.g. atmosphere)
  - Coupled earth system components
  
- ❑ R&D on simultaneous MDA performed **using operational model and DA system**, including GFS, RRFS/HRRR, HAFS, WoF, demonstrate great potential of such approach to better utilize observations and to improve NWP
  
- ❑ **Examples of research on MDA methodology development are introduced**
  - A new MDA solver (MLGETKF)
  - New methods to treat ensemble deficiency in MDA
  
- ❑ **Fundamental research is needed** to address challenges associated with the **multiscale DA** for **all NWP applications: short range, medium range and S2S predictions**

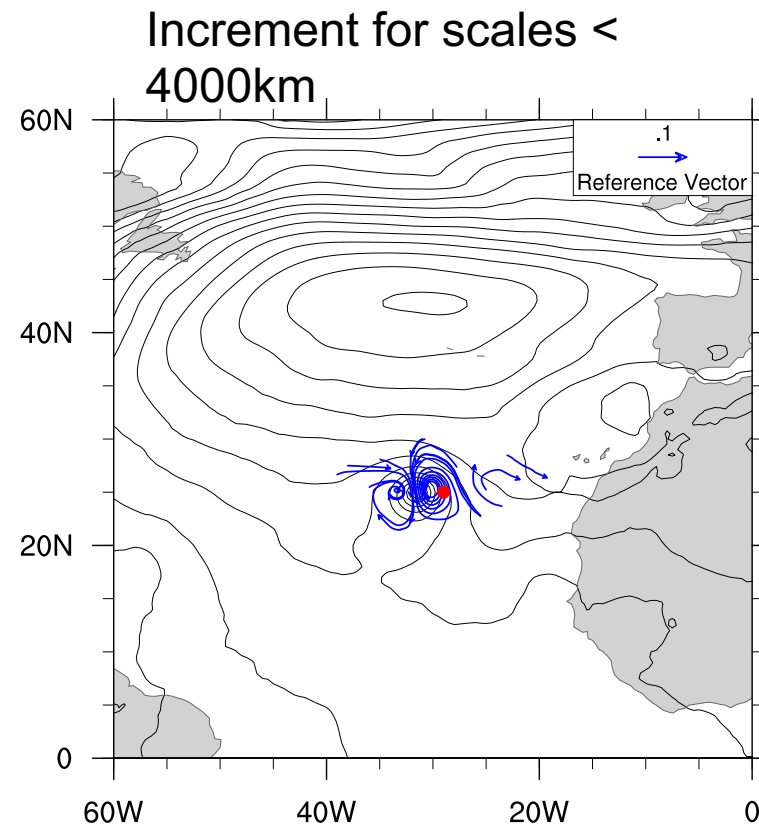
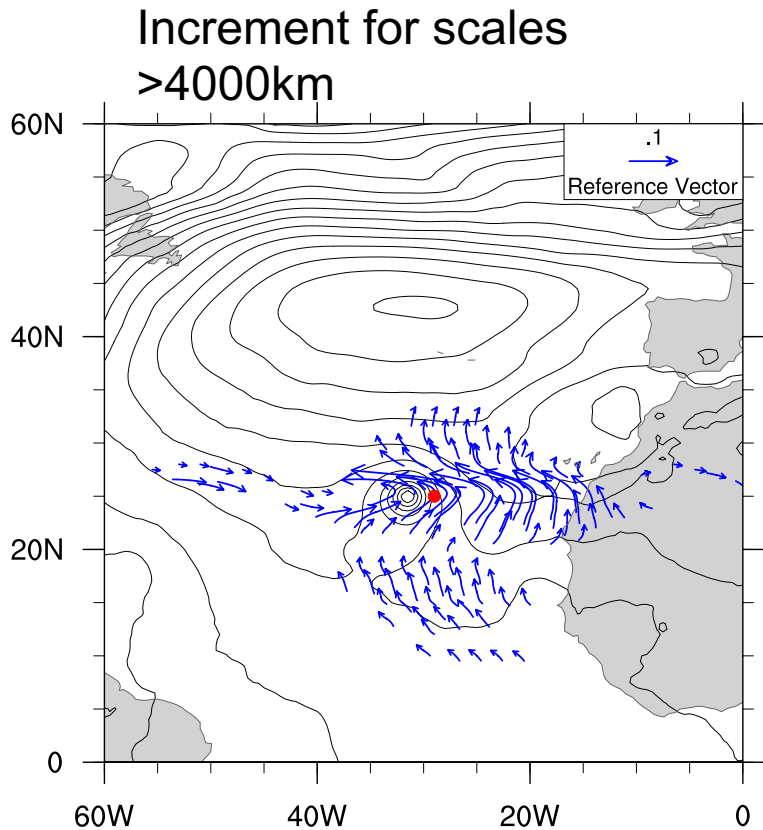


# Main References

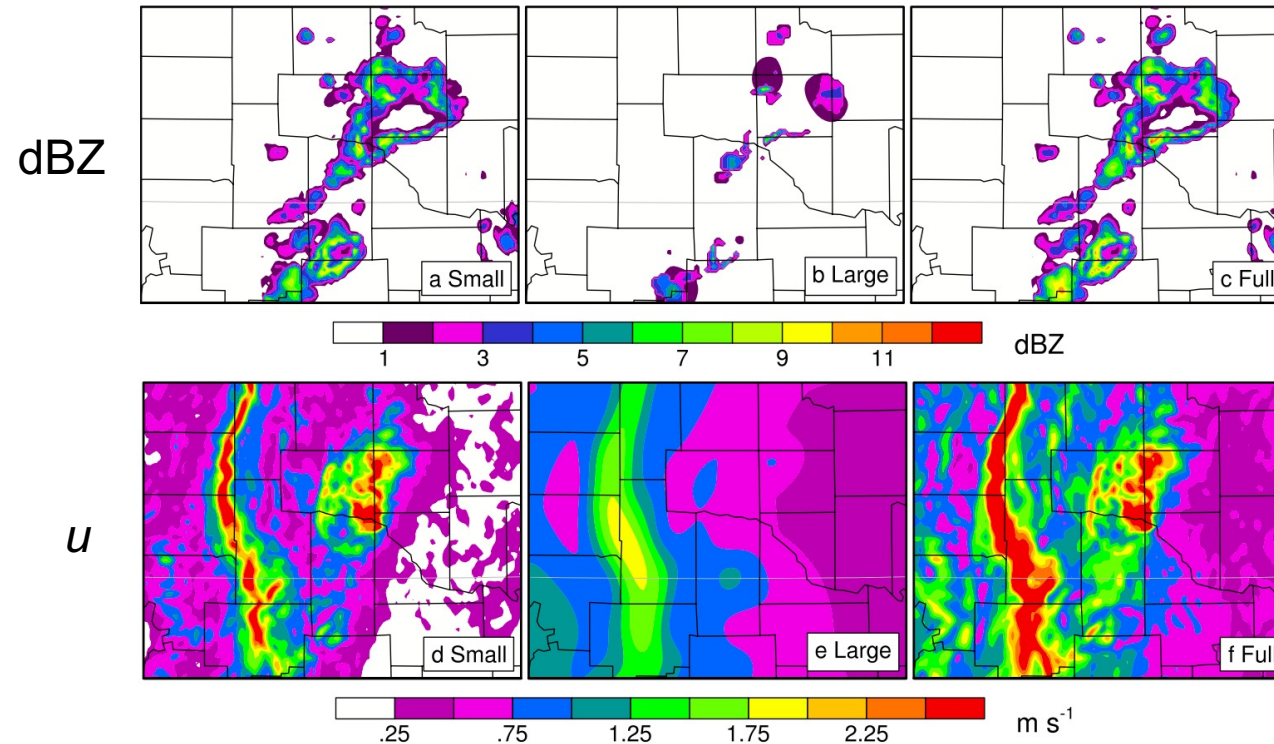


- Wang, X., H. Chipilski\*, C. H. Bishop, L. Satterfield, N. Baker and J. Whitaker, 2021: A Multiscale Local Gain Form Ensemble Transform Kalman Filter (MLGETKF), *Mon. Wea. Rev.*, <https://doi.org/10.1175/MWR-D-20-0290.1>
- Jones, E.\* and X. Wang, 2023a: A multi-resolution ensemble 4DEnVar with variable ensemble sizes to improve global and tropical cyclone track numerical prediction. *Mon. Wea. Rev.*, 151, 1145-1166.
- Jones, E.\* and X. Wang, 2023b: Flow-dependent vertical localization in hybrid 4DEnVar to improve global and tropical cyclone track numerical prediction. *Mon. Wea. Rev.*, to be submitted.
- Kay, J. K.\* and X. Wang, 2020: A multi-resolution ensemble hybrid 4DEnVar for global numerical prediction. *Mon. Wea. Rev.*, 148, 825-847.
- Huang, B.\*, X. Wang, D. Kleist, and T. Lei, 2021: Simultaneous Multi-scale Data Assimilation using Scale Dependent Localization in GSI-based Hybrid 4DEnVar for NCEP FV3-based GFS. *Mon. Wea. Rev.*, <https://doi.org/10.1175/MWR-D-20-0166.1>.
- Lu, X.\* and Wang, X. 2023: Simultaneous Multiscale EnVar with scale-dependent localization (SDL) in HAFS to improve hurricane predictions. *Mon. Wea. Rev.*, to be submitted.
- Wang, Y.\*, and X. Wang, 2017: Direct assimilation of radar reflectivity without tangent linear and adjoint of the nonlinear observation operator in the GSI-Based EnVar System: Methodology and experiment with the 8 May 2003 Oklahoma City tornadic supercell. *Mon. Wea. Rev.*, 145, 1447–1471, <https://doi.org/10.1175/MWR-D-16-0231.1>.
- Wang, Y.\* and X. Wang, 2021: Development of Convective-Scale Static Background Error Covariance within GSI-Based Hybrid EnVar System for Direct Radar Reflectivity Data Assimilation. *Mon. Wea. Rev.*, published.
- Wang, Y.\*, and X. Wang, 2023a: A Simultaneous Multiscale Data Assimilation using Scale- and Variable-Dependent Localization in EnVar to Improve Storm-Scale Ensemble-Based Data Assimilation and Forecasts: Methodology and Experiments for a Tornadic Supercell. *Journal of Advances in Modeling Earth Systems*, <https://doi.org/10.1029/2022MS003430>.
- Wang, Y.\* and X. Wang, 2023: Improving CONUS Convective-Scale Forecasting with Simultaneous Multiscale Data Assimilation: A Squall-Line Case Study, *Journal of Geophysical Research – Atmospheres*, submitted
- Xu\*, N., X. Wang and Y. Wang\*, 2023: Scale dependent inflation in multiscale ensemble based data assimilation. *Mon. Wea. Rev.*, to be submitted
- Yang, Y.\* and X. Wang, 2023: A Comparison of 3DEnVar and 4DEnVar for Convective-Scale Direct Radar Reflectivity Data Assimilation in the Context of Filter and Smoother, *Mon. Wea. Rev.*, accepted.

□ A simultaneous multiscale DA approach, as opposed to a sequential approach, allows all observations to correct all resolved scales at once (Wang X., 2021).



- A single obs. can correct multiple scales in simultaneous MDA
- Simultaneous multiscale DA also defines cross scale band error correlation

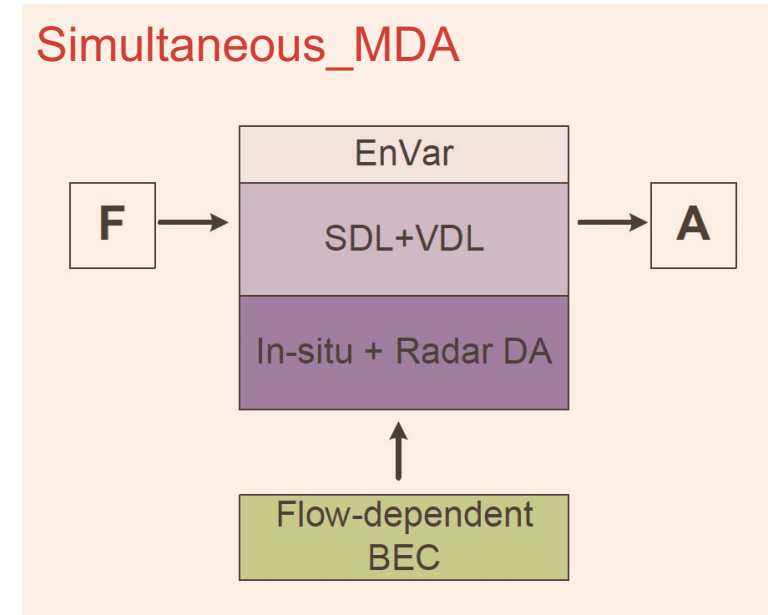
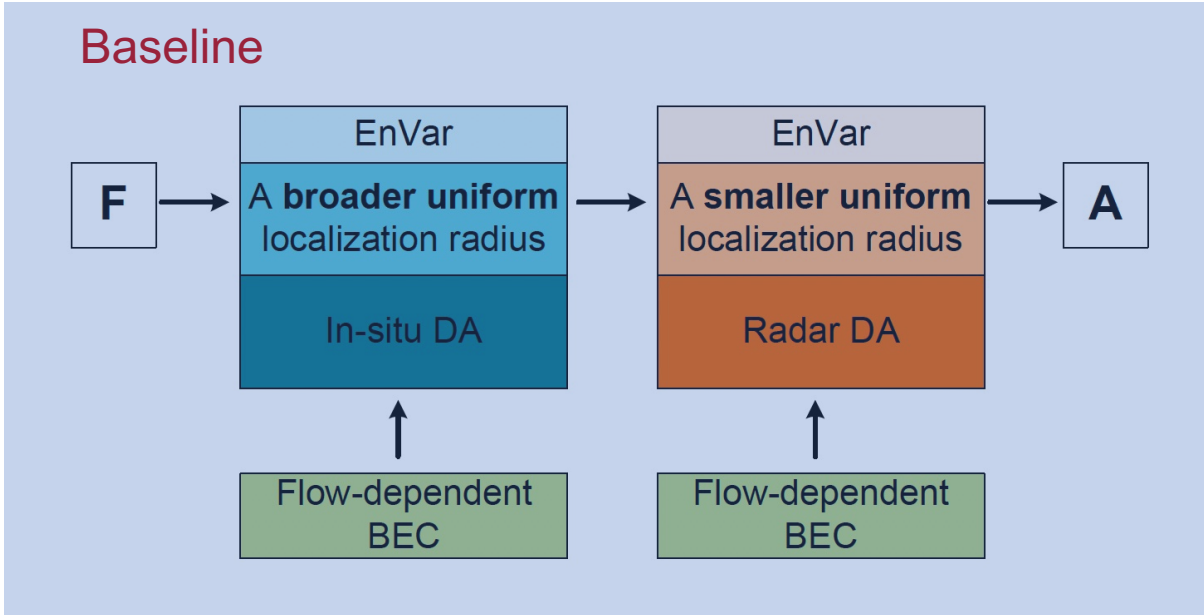


- A diffusion operator is applied to decompose scales for each ensemble perturbation.
- Uncertainty of the storm and small-scale low-level convergence are mostly concentrated at the decomposed small scale.
- Uncertainty of the environment-related fields are reflected by the large scale.



# Experiment design

## Model and DA configuration



Exps	Assimilation Strategy	Localization scales	
Baseline (Ope.-like)	Separate assimilation of in-situ and radar obs.	In-situ obs.	300 km
		Radar obs.	15 km
Simultaneous_MDA	Simultaneous assimilation of in-situ and radar obs.	Small scale	15 km: hydrometeors, and $w$
			60 km: $u$ , $v$ , $t$ , $q$ , and $ps$
		Large scale	60 km: hydrometeors, and $w$ 500 km: $u$ , $v$ , $t$ , $q$ , and $ps$

**Table 2***List of Experiments and Their Configuration of Horizontal Localization Radius*

Experiments	Horizontal localization radius
Exp-SSL	10 km for full-scale ensemble perturbations
Exp-SDL	10 and 60 km for all variables of small- and large-scale ensemble perturbations, respectively.
Exp-SDLVDL	10 km for all variables of small-scale ensemble perturbations; 15 km for $q$ , $w$ , $ql$ , $qr$ , $qs$ , $qi$ , $qg$ , and $dbz$ of large-scale ensemble perturbations; 60 km for $u$ , $v$ , $t$ , $ps$ of large-scale ensemble perturbations

# Key aspects of the algorithm

$$\mathbf{Z}^{ML} = (\mathbf{z}_1, \mathbf{z}_2, \dots, \mathbf{z}_{K_{ML}}) = (\mathbf{I} \quad \mathbf{I} \quad \dots \quad \mathbf{I}) \left( \mathbf{X}^{MS} \Delta \left[ (\mathbf{L}^{MS})^{\frac{1}{2}} \right] \right)$$

Modulated/expanded pseudo ensemble perturbations

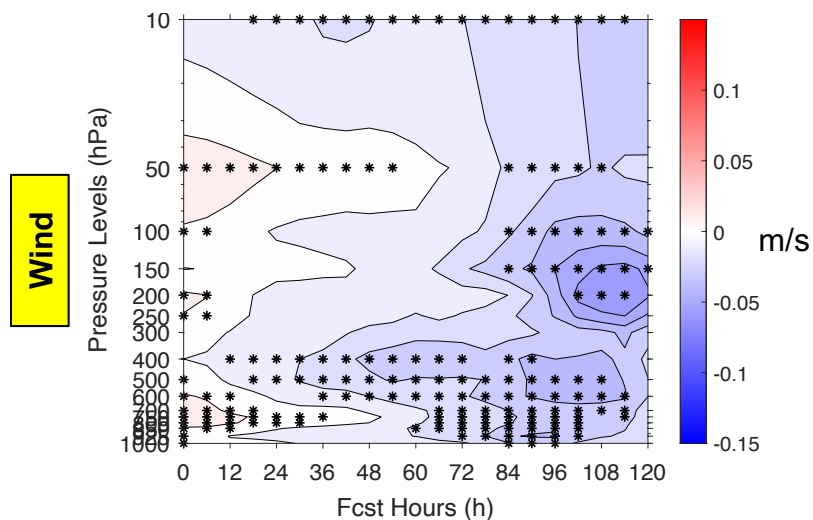
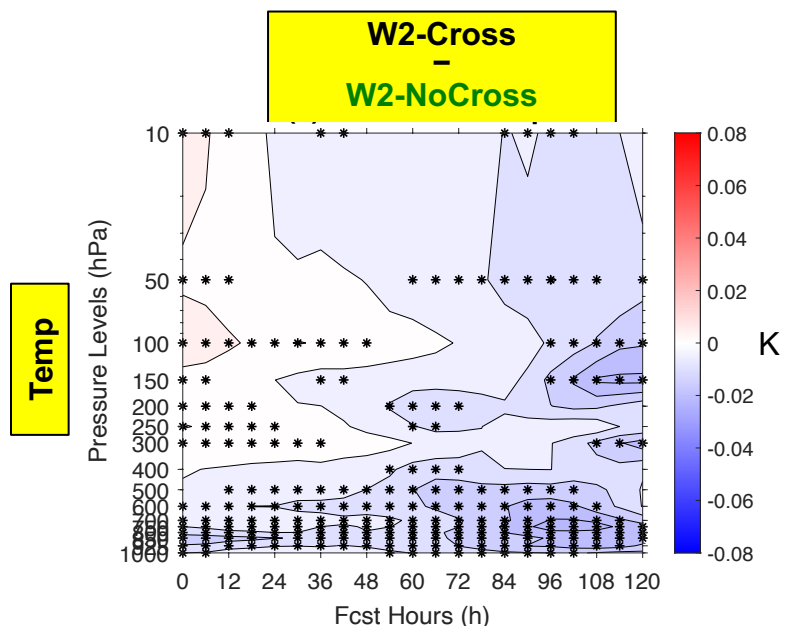
Scale decomposed raw perturbations

Multiscale model space localization

- Rapid creation of many pseudo ensemble perturbations in a local volume via a multiscale ensemble modulation procedure.
- The modulated ensemble intrinsically includes multi-scale model space localization and is used to update ensemble mean and perturbations.
- Multi-scale model space localization adopts scale-aware localization. In addition, localization of the ensemble covariances between different scales are defined and can be further modulated.
- MLGETKF only updates and propagates the original number of ensemble members.



# Impact of cross band correlation



RMSE difference between W2-Cross and W2-NoCross (blue/red → better/worse forecasts in W2-Cross)

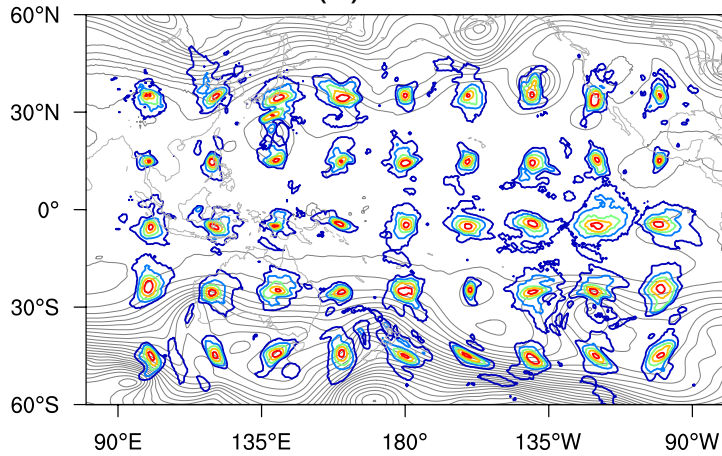
- W2-NoCross shows slightly better forecasts than W2-Cross within one day. This may benefit from the spatial averaging of ensemble covariances in W2-NoCross.
- Beyond one-day, W2-Cross in general shows more accurate forecasts than W2-NoCross, likely contributed by its higher degrees of retained heterogeneity of ensemble covariances and resultant analysis, and its more balanced analysis through partially including cross-waveband covariances.

Huang\*, Wang, et al. 2021

## Physical space visualization

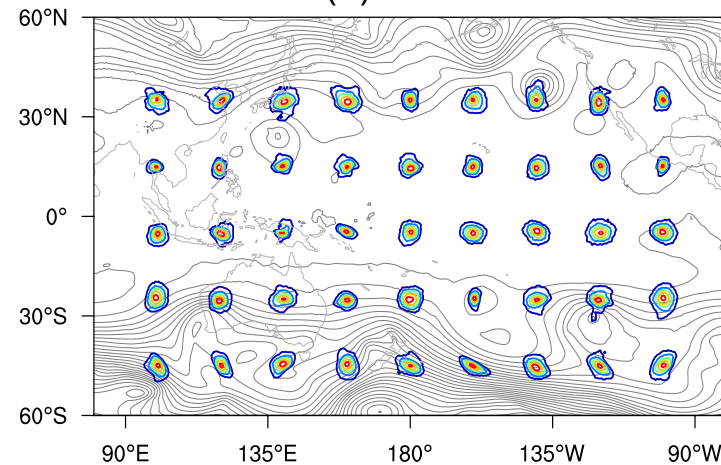
### Single large

(b) W1-1000



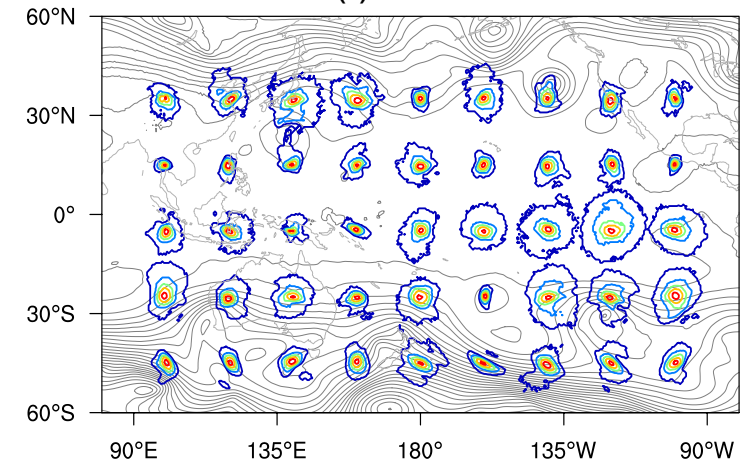
### Single small

(d) W1-300

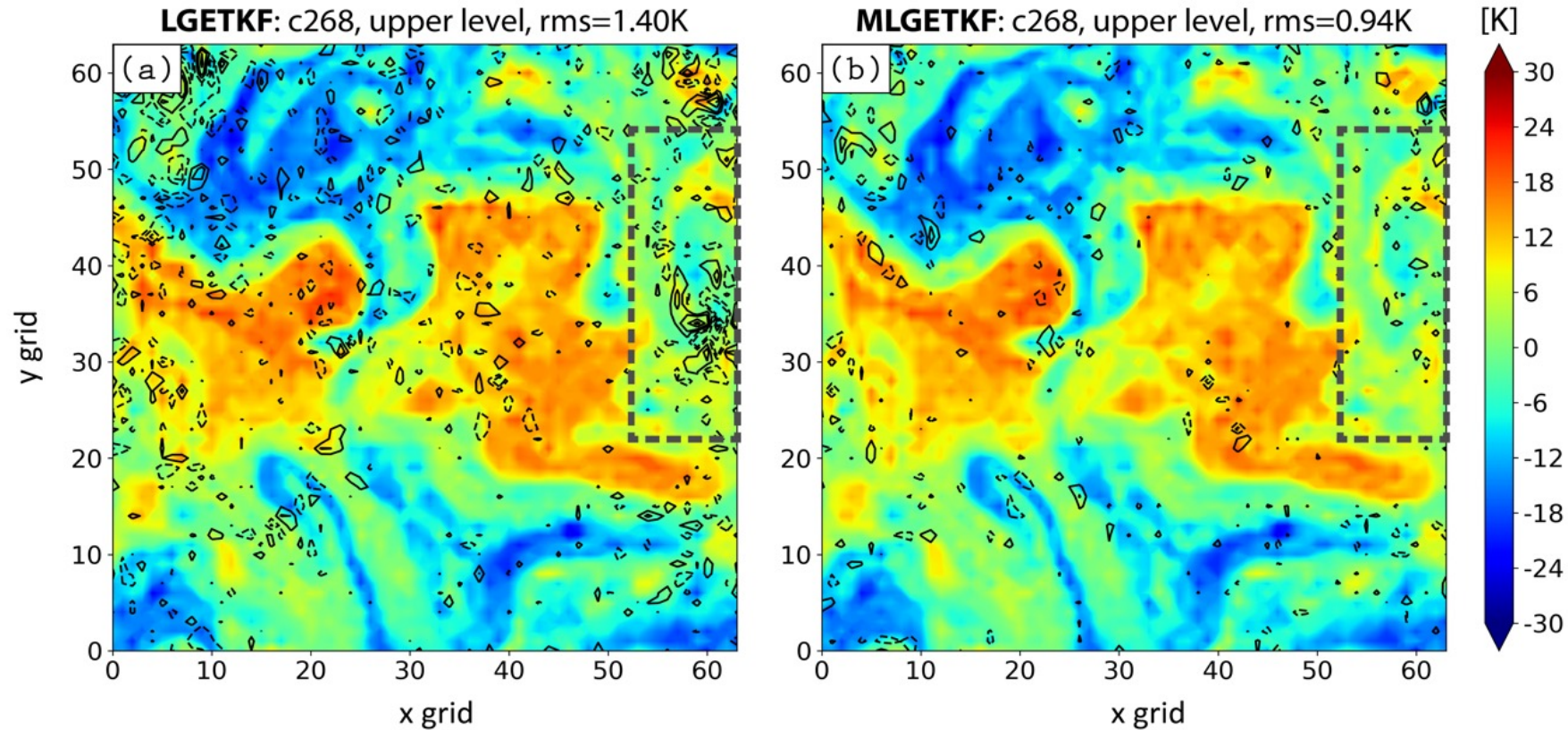


### Multiscale (MDA)

(f) W2-Cross



Huang\*, Wang et al. 2021



- MLGETKF not only shows skill in decreasing the small scale component of the analysis errors, but also is effective in suppressing the development of large scale, dynamical, high-amplitude analysis errors